Marine Geodesy
Publication details, including instructions for authors and subscription information:
http://www.tandfonline.com/loi/umgd20

Comparison of the Ku-Band Range Noise Level and the Relative Sea-State Bias of the Jason-1, TOPEX, and Poseidon-1 Radar Altimeters Special Issue: Jason-1 Calibration/Validation

O. Z. Zanifé [a], P. Vincent [b], L. Amarouche [a], J. P. Dumont [a], P. Thibaut [a] & S. Labroue [a]
[a] Collecte Localisation Satellite, Ramonville St. Agne, France
[b] Centre National d'Etudes Spatiales, Toulouse, France
Version of record first published: 21 Jun 2010.

To cite this article: O. Z. Zanifé , P. Vincent , L. Amarouche , J. P. Dumont , P. Thibaut & S. Labroue (2003): Comparison of the Ku-Band Range Noise Level and the Relative Sea-State Bias of the Jason-1, TOPEX, and Poseidon-1 Radar Altimeters Special Issue: Jason-1 Calibration/Validation, Marine Geodesy, 26:3-4, 201-238

To link to this article: http://dx.doi.org/10.1080/714044519

Marine Geodesy, 26: 201–238, 2003

ISSN: 0149-0419 print / 1521-060X online
DOI: 10.1080/01490410390255737

Taylor & Francis
Taylor & Francis Group

Comparison of the Ku-Band Range Noise Level and the Relative Sea-State Bias of the Jason-1, TOPEX, and Poseidon-1 Radar Altimeters

O. Z. ZANIFÉ

Collecte Localisation Satellite
Ramonville St. Agne, France

P. VINCENT

Centre National d'Etudes Spatiales
Toulouse, France

L. AMAROUCHE
J. P. DUMONT
P. THIBAUT
S. LABROUE

Collecte Localisation Satellite
Ramonville St. Agne, France

TOPEX/Poseidon is a well known success, with the operational altimeter (TOPEX) and the experimental one (Poseidon-1), providing data of unprecedented quality. However, there are two major differences between the TOPEX and Poseidon-1 radar altimeters on board TOPEX/Poseidon. The first is related to the estimated range noise; the second is linked to the sea-state bias (SSB) model estimates. Since the recent launch of the Jason-1 radar altimeter (also called Poseidon-2), we have been cross-comparing these three systems to better characterize each of them. Analyzing standard user products, we have found that Jason-1 is behaving like Poseidon-1 and thus shows the same observed differences when compared with TOPEX. A comparative analysis of their features was performed, starting from the on-board acquisition of the ocean return and ending with the ground generation of the high level accuracy oceanographic product. The results lead us to believe that the sources for these differences lie in both the waveform tracking processing and the presence or abscence of a retracking procedure whether on-board or on ground. Because Poseidon-1 and Jason-1 waveforms are retracked while TOPEX waveforms are not in the products distributed to the users, we have applied the same ground retracking algorithm to the waveforms of the three radar altimeters to get consistent data sets. The analysis of the outputs has shown that: (a) the noise level for the three radar altimeters is definitively the same, and (b) the source of the relative SSB between Jason-1 and TOPEX lies in the different behavior of the on-board tracking softwares.

Received 7 December 2002; accepted 12 September 2003.

This study could not have been completed without the work performed by several CNES and CLS young graduate students (D. Derrien, L. Amarouche, Y. Bertrand, C. L'Hermine, C. Durand, and A. Ollivier). We would like to thank also the CAL/VAL team at CLS for providing us with some of their internal results. Also, many thanks to N. Tran for the support and for the help in reading and correcting the manuscript. Finally a great thanks to G. Born, who has been very patient and who allowed us time to finish this article.

Address correspondence to O. Z. Zanifé, Collecte Localisation Satellite (CLS), 8-10 rue Hermès, 31526 Ramonville St. Agne, France. E-mail: ouan-zan.zanife@cls.fr

Keywords Jason-1, noise level, Poseidon-1, radar altimeter, retracking, sea state bias, TOPEX, tracker, waveforms

The Jason-1 satellite was successfully launched on 7 December 2001 by a Delta II rocket from the Vandenberg military base (CA, USA), to pursue the acquisition of valuable oceanographic data started by the TOPEX/Poseidon (T/P) mission in 1992 (Fu et al. 1994). Like the T/P mission, the Jason-1 mission is jointly conducted by CNES (Centre National d'Etudes Spatiales) and NASA (National Aeronautics and Space Administration). The payload (Perbos et al. 2003) is similar to its predecessor and consists of:

- a dual-frequency radar altimeter (Ku- and C-band), Poseidon-2 (hereafter designated as Jason-1);
- a three-channel radiometer, JMR (Jason Microwave Radiometer);
- two dual-frequency tracking systems, DORIS (Détermination d'Orbite et Radiopositionnement Intégrés par Satellite) and GPS TRSR (Global Positioning System Turbo Rogue Space Receiver); and
- a laser retro-reflector array.

To allow the verification and validation of the Jason-1 payload in ocean conditions similar to those seen by T/P, both satellites were placed on the same ground track, separated by about 72 s, Jason-1 ahead of T/P. This period lasted from January to August 2002. During this period, the Poseidon-1 radar altimeter of the T/P satellite was switched on one time in July 2002 during cycle 361 (corresponding to Jason-1 cycle 18), and the TOPEX altimeter was active during the remaining cycles. This gave the unique opportunity to compare the performances of the three radar altimeters (Jason-1, TOPEX, and Poseidon-1) in very similar ocean and environmental conditions.

The three major parameters measured by a radar altimeter are the distance from the satellite to the sea surface, the distance between the trough and the crest of the waves, and the backscatter power; they are, respectively, related to the topography of the ocean (sea surface height, SSH), significant wave height (SWH), and wind speed (WS) (Chelton et al. 1989, 2001). From these measurements, the on-board and ground processing allows the retrieval of high level accuracy oceanographic products and their distribution to users worldwide.

The error budget for the Ku-band SSH parameter for TOPEX, Poseidon-1, and Jason-1 is given in Table 1 for standard conditions (2 m SWH and 11 dB backscatter coefficient or sigma0) using 1 s averaged data.

As far as the altimeter range is concerned, the major contributors to the error budget are the altimeter noise level and the sea-state bias (SSB), which is the combination of the electromagnetic bias (EMB), the tracker bias, and the skewness. As one can note on Table 1, Poseidon-1 seems to have a higher noise level (2 cm) than TOPEX (1.7 cm). Even if the error estimations for the SSB are the same for both TOPEX and Poseidon-1, the SSB models expressed as a function of SWH are significantly different; their difference is estimated to be about 1 to 1.5% of SWH. These differences have been and still are the subjects of several studies looking for their sources. The goal of this article is to revisit the noise and relative SSB topics, with Jason-1 considered as the reference mission in this study.

First, a brief review of the current status of the various estimates of the noise level and the SSB will be given. This will highlight the differences between the three radar altimeter systems. These will then be described and their major differences will be discussed. This will enable us to point out and discuss the possible sources of these differences. To ensure a meaningful comparison, data from the three instruments are then reprocessed consistently.

TABLE 1 Sea Surface Height Error Budget of the TOPEX, Poseidon-1, and Jason-1 System (The Values for TOPEX and Poseidon-1 are Extracted from Fu et al. (1994). The Values for Jason-1 are Issued from Ménard et al. (2003) and are relative to the IGDR Product.)

	TOPEX (cm)	Poseidon-1 (cm)	Jason-1 (IGDR) (cm)
Altimeter range			
Altimeter noise	1.7	2.0	1.6
Tracker bias	—	—	—
EM bias	2.0	2.0	2.0
Skewness	1.2	1.2	—
Ionosphere	0.5	1.7	0.5
Dry troposphere	0.7	0.7	0.7
Wet troposhere	1.1	1.1	1.2
Total altimeter range	3.2	3.7	3.0
POD			
*Radial orbit height	2.5	2.5	2.5
Sea surface height			
Single-pass	4.1	4.5	3.9

*The original value of the POD accuracy for TOPEX and Poseidon has been replaced by the one given in Chelton et al. (2001).

The reprocessing procedure and resulting data sets will be presented in detail. Results of the comparison of the three data sets will be shown and discussed.

Current Knowledge About Noise and SSB

This section presents several noise and SSB estimations derived from various methods by different authors.

Noise

Using a high-pass filtering technique applied to the 1 Hz SSH, Tran et al. (2002) derived the 1 Hz noise level for the TOPEX, Poseidon-1, and GFO altimeters. Their results are similar to those reported in Table 1, and a 2.5 cm figure appears for GFO. Using an alternative technique based on a low pass filter applied to the high rate sea level anomalies (SLA) of Jason-1 (20 Hz) and Poseidon-1 (10 Hz), Dorandeu et al. (2002) found that the 1 Hz noise level is identical for both altimeters and is equal to 1.6 cm. This value confirmed the one found by Zanifé et al. (2001), using spectral analysis on Poseidon-1 20 Hz data. Both Dorandeu and Zanifé results assume that the high rate data are uncorrelated.

The CAL/VAL team at CLS (Dorandeu et al. 2001) performs a systematic quality control checking and a long-term monitoring of the T/P data on behalf of CNES on an operational basis. This quality control has been extended to Jason data after launch. Among the parameters that are monitored, the standard deviation of the linear fit over 1 s of the high rate Ku range data (respectively 10 Hz Ku for TOPEX and 20 Hz for Poseidon-1 and Jason-1) is one of them. This parameter is provided through its mean value computed on a cycle basis; it is displayed in Figure 1 as a function of cycle number for the overlapping cycles of the T/P and Jason-1 missions. While it is often simplified as an instrument noise estimate, it shows that the TOPEX altimeter provides measurements with smaller noise than Poseidon-1 and Jason-1 altimeters.

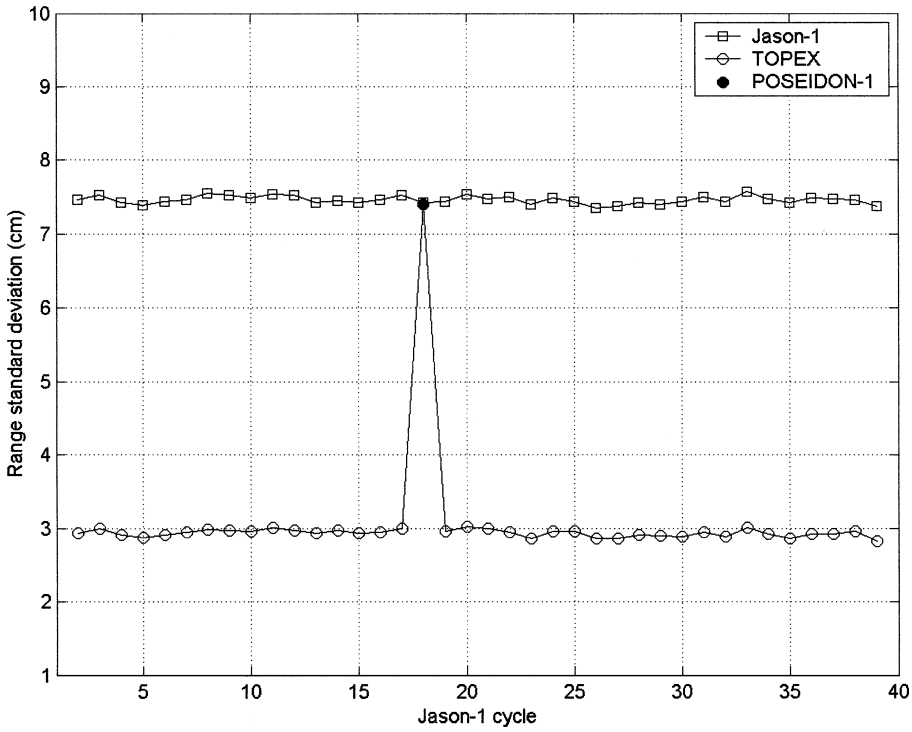

FIGURE 1 Cycle average of the high rate Ku-band range standard deviation for TOPEX (10 Hz), Poseidon-1 (20 Hz), and Jason-1 (20 Hz).

From Figure 1, the TOPEX 10 Hz Ku-band range rms from the fit is equal to 3 cm while the Poseidon-1 and the Jason-1 figures are both equal to 7.5 cm. These values can be approximately related to the 1 Hz values using the decorrelation assumption of the high rate data over 1 s. If full decorrelation is assumed—which is not necessarily the case (see Noise Level Results and Analysis section)—TOPEX values should be divided by square root of 10 and the Poseidon-1 and Jason-1 by square root of 20, resulting in 0.95 cm for TOPEX and 1.7 cm for Poseidon altimeters.

All the previous figures seem to indicate that the various altimeters have very different noise levels. One of the goals of this article is to show that, when processed homogeneously, the data from the three altimeters exhibit the same noise level.

SSB

As far as the SSB is concerned, different methods can be used to derive empirical models (Gaspar et al. 1994, 1998, 2002). We recall here the results obtained with the BM4 model fitted on the three altimeters data. Even if such a model gives the wind- and wave-related variations, we are here interested in the SSB dependency along the waves, and the wind speed dependency is neglected for a raw approximation of the SSB.

Among the parameters that the CAL/VAL team monitors is the first order coefficient of the BM4 model (see Figure 2). While the value for TOPEX is about -2.5%, the corresponding value for either Poseidon-1 and Jason-1 is about -3.75%, exhibiting a difference of 1.25% of SWH.

Note that the values shown for Poseidon-1 are obtained after removing a normalization correction, as reported by AVISO (1996). This normalization process has been performed

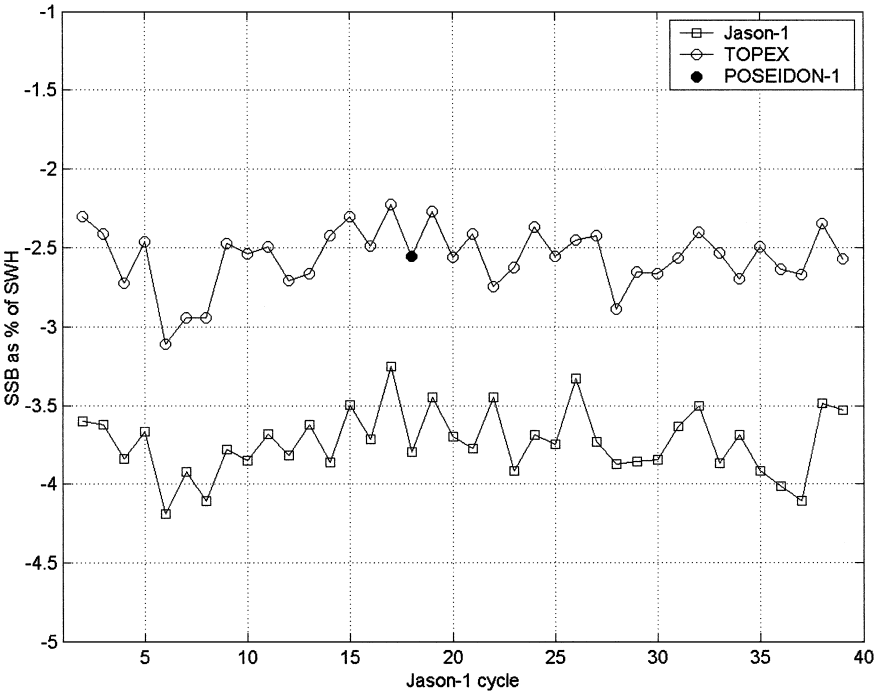

FIGURE 2 Cycle average of the first order coefficient of the SSB for TOPEX, Poseidon-1, and Jason-1.

to get homogeneity between TOPEX and Poseidon-1 user products, leading to separate the −3.7% SWH Poseidon-1 SSB in a −2 to −2.5% SWH BM4 SSB similar to TOPEX plus a −1.7% SWH additional normalization correction incorporated in the sum of the instrumental corrections.

The second goal of this article is to look for the origin of the relative SSB differences between all three altimeters.

Radar Altimeter System Comparison

Overview

The figures given in the previous section for the noise level and SSB models have been obtained from the user products delivered by AVISO and PODAAC. These are the MGDR for TOPEX and Poseidon-1 and the IGDR for Jason-1. Below is an overview of the systems that generate these products.

Let's consider the radar altimeter system from the on-board emission of a pulse towards the ocean and up to the computation of the range from the satellite to the ocean surface. The system includes the on-board acquisition of the waveforms (including tracking) and the ground processing of the telemetry up to level 2, that is:

- decommutation, transfer function, and quality control (also known as level 1.0 processing);
- instrumental corrections (also known as level 1.5 processing); and
- geophysical corrections plus retracking and SSB (also known as level 2.0 processing).

Level 1.0 processing is specifically attached to an instrument and its telemetry. The transformation of the telemetry data into engineering data does not affect the precision/

accuracy of the data. We will thus consider that these operations do not provide an explaination for the noise/SSB questions.

The level 1.5 corrections applied to the altimetric parameters do have an impact on the precision/accuracy of the data. Nevertheless, these corrections are governed by well established equations (Doppler effect, USO drift, etc.) which affect the precision/accuracy in the same manner for all altimeters. Here again, this processing step does not provide an explaination for the questions raised.

As far as the environmental and geophysical algorithms are concerned, the T/P experience resulted in their quasi standardization (Dumont et al. 2001), except for the retracking and SSB algorithms. Thus, apart from these two algorithms, we will consider that the level 2 processing does not introduce any difference in the data of the three systems. The retracking algorithm and its associated algorithms (corrections of the waveforms for the low pass filter effects, look up tables derived either from numerical simulator or hardware test bed) are the only ones that introduce a significant difference.

Besides the ground retracking algorithm, another upstream technical subsystem that could lead to significant differences between altimeter systems is the on-board waveform acquisition and the on-board processing. We will now look into them.

On-Board Waveform Acquisition and Tracking

The major steps of the acquisition and tracking of the waveforms are as follows. At regular intervals defined by the Pulse Repetition Frequency (PRF) (see Table 2), frequency linearly modulated pulses are transmitted by the altimeter towards the earth's surface. After reflection on the surface, the pulse is received back on board and mixed with a pulse similar to the emitted one which has been triggered by the tracker information. The mixed pulse, which is referred to as the "individual echo," provides a sampled measurement of the return power as a function of time, distance, or frequency. In order to reduce the statistical fluctuations (speckle) which affect the individual echoes and to perform real-time tracking (i.e., to maintain the signal inside an analysis window as far as range and power are concerned), these echoes are averaged on board over a period which corresponds to the altimeter duty cycle (typically 50 ms). The resulting signal is referred to as an "averaged echo" or a "waveform." It is processed by the on-board tracking to derive the range and the power. In the TOPEX case, the SWH information is also extracted. These data are then used as inputs of the tracking loop during the duty cycle that follows.

TABLE 2 Radio Frequency Values of the TOPEX, Poseidon-1, and Jason-1 Systems

	TOPEX	Poseidon-1	Jason-1
RF features			
Frequency (GHz)	13.6	13.65	13.575
Pulse duration (ms)	102.4	105.6	105.6
Bandwidth (MHz)	320	320	320
PRF (Hz)	4200	1718	1800
Pulses number:	228	86	90
On-board waveform rate (Hz)	20	20	20
On-board waveform samples	128	64	128
On-board sample resolution:	3.125 ns or 46.84 cm	3.125 ns or 46.84 cm	3.125 ns or 46.84 cm
On-board reference sample index:	32.5	32	44
Antenna beamwidth (deg.):	1.08	1.1	1.28

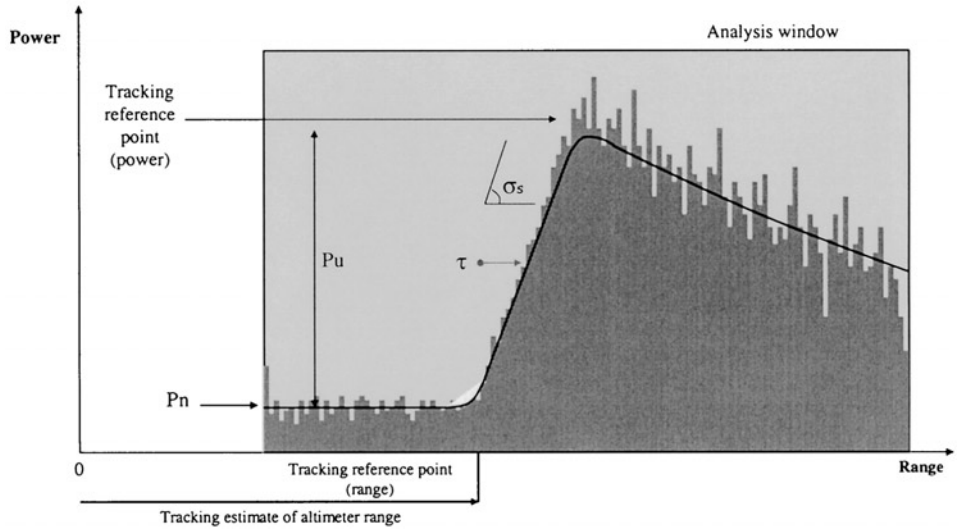

FIGURE 3 Waveform in tracking window.

The theoretical shape of an echo over an ocean surface is represented in Figure 3 (the dotted signal represents the speckle, that is, the statistical fluctuations affecting the echo). Such a radar echo is characterized by the following main parameters:

- the epoch or time delay τ, that is, the position of the signal in the analysis window with respect to the tracking reference point (τ represents the tracking error on the estimate of the altimeter range);
- the amplitude of the useful signal in the analysis window, P_u;
- the slope of the leading edge, which is a function of the standard deviation of heights, σ_s, that can be related to SWH (assuming a Gaussian distribution of ocean heights);
- the level of thermal noise, P_n; and
- other parameters, such as mispointing (ξ) and skewness (λ_s).

The acquisition and tracking functions are carried out by two subsystems. The first one performs acquisition of the waveforms, this is the Radio Frequency Unit (RFU). The second one processes the waveforms, this is the Processing and Control Unit (PCU). In this article, the PCU will be limited to the on-board tracker software.

RFU

The parameters characterizing the RFU are given in Table 2. They are extracted from Escudier et al. (2000), Hayne et al. (1994), Raizonville et al. (1991), and Zieger et al. (1991). From one system to the other, the RFU features are very similar. The significant differences are related to the number of samples of the waveforms, the antenna beamwidth, and the pulse repetition frequency. The first two do not have any significant impact on noise and SSB. The difference in the value of the antenna beamwidth is due to the physical size of the antenna. While the number of samples for Poseidon-1 is half that of TOPEX and of Jason-1, these samples are the ones containing the information needed to extract the altimetric parameters.

The major differences between TOPEX, Poseidon-1, and the Jason-1 radar altimeters are the PRF and the related pulse number parameter. While close PRF values have been given to Poseidon-1 and Jason-1, respectively 1718 Hz and 1800 Hz, the one used for

TOPEX is a factor of two above these values. Studies performed by Walsh et al. (1982), and Rodriguez et al. (1994a) have shown that this increase of the PRF should not affect the performances in standard conditions; however, for extreme sea-state conditions (SWH greater than 8 m), the higher PRF allows a better sampling of the signal. Therefore, it seems very unlikely that the PRF difference is responsible for the difference in noise or SSB over most of the SWH range variation.

On-Board Tracker

The tracking function consists of keeping the waveforms well centered in range and power in the analysis window (see Figure 3). This is performed by the first- or second-order filter closed loops. The parameters derived are the tracker range, the Automatic Gain Control (AGC), and a parameter related to SWH.

The values of the on-board tracker parameters are given in Table 3 (Carayon et al. 2003, Marth et al. 1993, Raizonville et al. 1991, Zieger et al. 1991).

The tracker equations are given below for the tracker range (h_{n+2}) and the tracker range rate (r_{n+2}) at the current duty cycle ($n + 1$) for, respectively, TOPEX and Poseidon instrument series:

TOPEX:

$$\begin{cases} h_{n+2} = h_{n+1} + r_{n+1} + \alpha\varepsilon_{h_n} \\ r_{n+2} = r_{n+1} + \beta\varepsilon_{h_n}, \end{cases} \tag{1}$$

and

Poseidon-1 and -2

$$\begin{cases} h_{n+2} = h_{n+1} + r_{n+1} + CL_n \quad \text{with } CL_n = \alpha\left(\varepsilon_{h_n} - CL_{n-1}\right) \\ r_{n+2} = r_{n+1} + \beta\varepsilon_{h_n}, \end{cases} \tag{2}$$

where α and β are the gains of the filter, which values can be found in Table 3, and ε_{hn} is the range error as measured by the tracker. This error is the deviation of the waveform reference point (see Figure 3) position from the reference point of the analysis window. It is computed using the energies of fixed windows for Poseidon-1 and Jason-1, and adaptive windows for TOPEX.

Although the two sets of equations are very similar, several differences appear. The first one is the CL_n term for the Poseidon tracker. Its purpose is to compensate the system due to the two duty cycle delay. The second one is relative to the β gain values that can be found in Table 3. The impact of these two differences is shown in Figure 4, where the frequency analysis of the two filters have been drawn. An additional filter called "TOPEX mod" has been added to this plot to show the impact of a β gain change from 1/64 to 1/128.

From Figure 4, two observations can be made. On the one hand, the comparison of the TOPEX filter with its modified version (β = 1/128 instead of 1/64) shows that the transfer function is the subject of no distortion for frequencies higher than 2 Hz, whereas below this frequency we can see that the bandwidth is reduced by a factor of 1/3. The lower β value associated with Poseidon keeps the level of the transfer function closer to 1 and increases the acceleration lag of the tracker. On the other hand, the comparison of Poseidon and TOPEX transfer functions shows that the compensation term significantly reduces the signal at intermediate frequencies and attenuates it to a lesser extent at high frequencies. Thus, these features are potential candidates for explaining the issues on noise and SSB.

The third difference between the tracker algorithms is the procedure used to compute the range error. Following Chelton et al. (1989, 2001), we recall that the range error computation

TABLE 3 Tracker Parameters of the TOPEX, Poseidon-1, and Jason-1 Systems

	TOPEX	Poseidon-1	Jason-1
Tracker			
Range error computation	Adaptative windows	Fixed windows	Fixed windows
Samples used	5 to 56	6 to 58	18 to 71
Estimated parameters	Range, AGC, and SWH	Range and AGC	Range and AGC
Rate (Hz)	20	20	20
Range (values of the filter gain)	Second-order filter (1/4, 1/64)	Second-order filter (1/4, 1/128)	Second-order filter (1/4, 1/128)
AGC (values of the filter gain)	First-order filter (0.3)	First-order filter (0.5)	First-order filter (0.5)
SWH	Ratio of energy	/	/

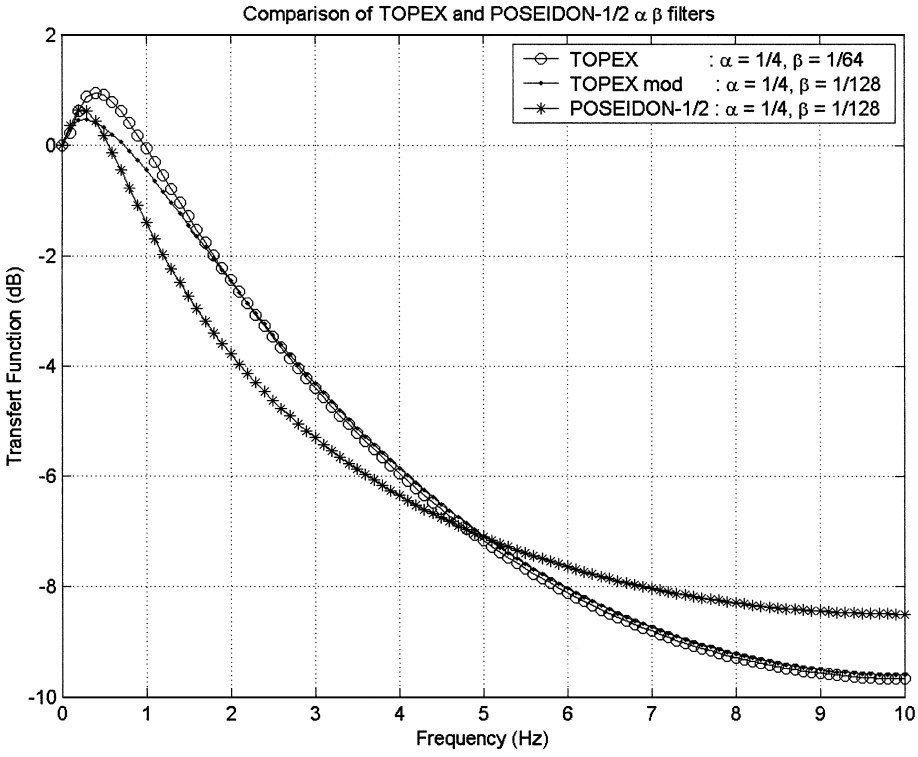

FIGURE 4 Comparison of TOPEX and Poseidon-1/2 (α, β) filter.

is based on the comparison of the energies in different parts of the waveform and then translated into range. In the case of Poseidon instruments, because a retracking processing (either on-board or on the ground) was intended, a simple tracker such as the split gate tracker (or fixed windows) has been used, since any error introduced by the tracker could later be removed by retracking the waveforms. On the other hand, the design of the TOPEX tracker algorithm is more sophisticated; it includes the two functions consisting in tracking the waveforms and estimating the parameters. This leads to the design of an adaptive windows tracker. As a consequence, there is a need to compute a quantity related to the SWH in order to adapt the tracking windows according to the received signal.

For Poseidon-1 and Jason-1, the range error equation is given by:

$$\varepsilon_{hn} = Scale\left[k^* \frac{(E_3 - E_1)}{2} - (E_2 - E_1)\right], \tag{3}$$

with E_1, E_2, and E_3 representing the average power ($E_j = \frac{1}{N_j} \sum_i V_i$) in the thermal noise, leading edge, and trailing windows, respectively. The Poseidon-1 windows are defined by the following samples: (a) samples 6 to 19 for the noise, (b) samples 20 to 44 for the leading edge, and (c) samples 45 to 58 for the trailing edge. For Jason-1, the definition of the windows is the same, except that they have been moved by 12 gates to account for the change of the reference point from 32 to 44. The k factor (equal to 1.2 for Poseidon-1 and 1.116 for Jason-1) has been introduced to account for the decay in the trailing edge due to the antenna pattern. The *Scale* parameter (equal to 7.32 cm/unit power) is used to convert the difference of power into range.

For TOPEX, the range error formula is:

$$\varepsilon_{hn} = Scale[k^{*}AGC\_Gate - Middle\_Gate_{m}], \tag{4}$$

where *Scale* and k have the same meaning as in the Poseidon algorithm. *AGC_Gate* is the average power between samples 17 and 48 and $Middle\_Gate_m$ is the averaged power of five windows that encompass the leading edge. The choice of the parameter m is performed by the SWH algorithm (see Chelton et al. 1989, 2001). Values associated with the TOPEX tracker algorithm can be found in Chelton et al. (2001), Marth et al. (1993), and in Zieger et al. (1991).

In order to compare the altimeters in identical conditions, it is necessary to apply a retracking procedure with similar configurations to the TOPEX, the Poseidon-1, and the Jason-1 data.

Ground Retracking

The retracking function consists of the estimation of τ, P_u, and σ_s (or SWH). The final range estimate will be the combination of the tracking range estimate and the epoch τ. The backscatter coefficient of the overflown surface (and hence the wind speed) is derived from the tracking power estimate (AGC) and the amplitude (P_u).

These estimations are performed by making the measured waveform coincide with a return power model according to weighted Least Square Estimators derived from Maximum Likelihood Estimators (Dumont 1985; Rodriguez et al. 1988). Assuming decorrelation of the sample noise in each waveform and decorrelation from one individual echo to the other, an iterative solution is obtained by developing the total cost function in a Taylor series at the first order from an initial set of estimates. This estimator is also called the MMSE (minimum mean square estimator), and the estimates are given by the following equation:

$$\theta_{m,n} = \theta_{m,n-1} - g(BB^{T})^{-1}_{\theta_{m,n-1}}(BD)_{\theta_{m,n-1}}, \tag{5}$$

where $\theta_{m,n}$ is the estimated parameter at iteration n, m is the index of estimated parameters, and g is the loop gain (varying between 0 and 1). The matrix of weighted partial derivatives (B) and the vector of weighted differences (D) are given by:

$$B_{m,k} = \frac{1}{Pu}\frac{\partial \bar{V}_k}{\partial \theta_m} \quad \text{and} \quad D_{k,1} = \frac{\bar{V}_k - V_k}{Pu}, \tag{6}$$

with k = sample index, $\bar{V}_k$ = model waveform sample k, V_k = measured waveform sample k, and Pu = estimated power. The original weight $1/\bar{V}_k$ of the Weighted Least Square Estimators method has been replaced by $1/Pu$ for the three following reasons: (a) to avoid giving to the noise region, which contains no signal, too much weight; (b) to ensure that all samples have the same weight; and (c) to normalize the residual, thus providing more robust estimates.

The analytic ocean return model is the one, first given by Brown (1977) and refined by Hayne (1980), in which a fixed skewness has been included. Given the high stability of Poseidon-1 and Jason-1 altimeter Point Target Responses (PTR) (Vincent et al. 2003; Zanifé et al. 2001), it is possible to model them using one central Gaussian only. If the long-term monitoring of the PTR shows a significant change through time, it will be possible to correct for it through retracking by modeling the PTR using several Gaussians.

The convergence criterion of the iterative procedures (as it is implemented in the ground processing segment of the mission) is slightly different for Poseidon-1 and Jason-1. For Poseidon-1, it is based on the simultaneous stability of the three altimetric parameters on two consecutive steps. For Jason-1 the function of merit χ^2 also called MQE (mean quadratic error = average of the squared difference between the samples and the fit), which is defined by:

$$\chi^2 = \frac{1}{N} \sum_i \left(\frac{V_i - Vm_i}{Pu} \right)^2, \tag{7}$$

is used. And the solution is considered to be reached if the differences of the χ^2 computations are below a given threshold after three consecutive steps.

Table 4 presents the characteristics of the Poseidon-1 and Jason-1 retracking algorithms used in the T/P and Jason-1 ground segments. Related algorithms are also listed.

From Table 4, the differences between Poseidon-1 and Jason-1 retracking algorithms are the following:

- estimation of SigmaC (combination of SWH and impulse response of the altimeter) for Jason-1 and SWH for Poseidon-1,
- convergence criteria,
- maximum number of iterations, and
- samples used.

The evaluation of these differences is given in the next section, where we describe how all data have been reprocessed to get an homogeneous data set for all three altimeters.

Data Set and Data Processing

Data Set

Jason-1 data from cycles 17 and 18 (end of June, beginning of July 2002) are used with simultaneous T/P data from cycles 360 (TOPEX) and 361 (Poseidon-1). About 218 passes out of the 254 that comprise a cycle have been selected and represent about eight days of data: passes 007 to 019, 024 to 031, 033 to 040, 044 to 056, 068 to 095, 097 to 173, 176 to 240, 246 to 251. This amount of data is statistically meaningful to get valid stable results for noise as well as for the relative SSB of the three altimeters versus SWH.

Data Processing

To compare the data of the three radar altimeters in a consistent way, their waveforms have been retracked using identical algorithms. The detailed retracking configurations for each data set are given in Table 5. They differ only by the samples that were used; they are the same as the ones used by the on-board trackers and represent the same portion of the waveform for each instrument. Furthermore, Poseidon-1 and Jason-1 20 Hz waveforms have been averaged two by two before retracking, as is done for TOPEX. TOPEX waveforms are those from the SDR files delivered by the T/P project team. Jason-1 waveforms are from the SGDR products available from the Jason-1 project. Poseidon-1 waveforms are from the SSALTO ground segment in the form of the so-called MEGA files.

In the following sections and paragraphs, this retracking procedure will be called as the "OZZ" retracking.

TABLE 4 Mission Ground Segment Retracking Parameters of the TOPEX, Poseidon-1, and Jason-1 Systems

	TOPEX	Poseidon-1	Jason-1
Ground retracking			
Type	No	Iterative MMSE	Iterative MMSE
Samples used	/	5 to 60	14 to 116
Estimated parameters	/	Epoch, Power, and SWH	Epoch, Power, and Sigma_C
Rate (Hz)	/	20	20
Gain of the iterative	/	(1.0, 1.0, 1.0)	(1.0, 1.0, 1.0)
Convergence criteria	/	Param	MQE
Skewness	0.1	0.1	0
Minimum number of iterations	/	1	3
Maximum number of iterations	/	10	25
Look up tables	Yes	No	Yes
Acceleration correction	Yes	Through retracking	Through retracking
Correction of filter effects	Through look up tables	Through retracking	Through retracking
Normalization bias	No	Yes	No

To evaluate the impact of the differences listed in the Ground Retracking section, two comparisons between retracked data (using Jason-1 data of pass 13 cycle 18) have been performed:

- Poseidon-1 configuration against OZZ configuration, in order to evaluate the impact of the first three differences listed in the Ground Retracking section; and
- Jason-1 configuration against OZZ configuration, to evaluate the impact of the fourth difference of that same section, e.g. the samples used.

TABLE 5 Retracking Parameters Settings for the TOPEX, Poseidon-1, and Jason-1 Systems

	TOPEX	Poseidon-1	Jason-1
Samples used	5 to 56	5 to 56	18 to 70
Center sample	32.5	32	44
Waveforms rate (Hz)	10	10	10
Filter	Official one (Hayne et al. 1994)	Mission one	From LTM (Average over 20 cycles)
Antenna beamwidth	1.08	1.1	1.28
Skewness coefficient	0	0	0
Max number of iterations	25	25	25
Gains for the retracking	(1,1,1)	(1,1,1)	(1,1,1)
Coefficient for SigmaP	0.513	0.513	0.513
Convergence criteria	MQE	MQE	MQE
Threshold	5.00E-04	5.00E-04	5.00E-04

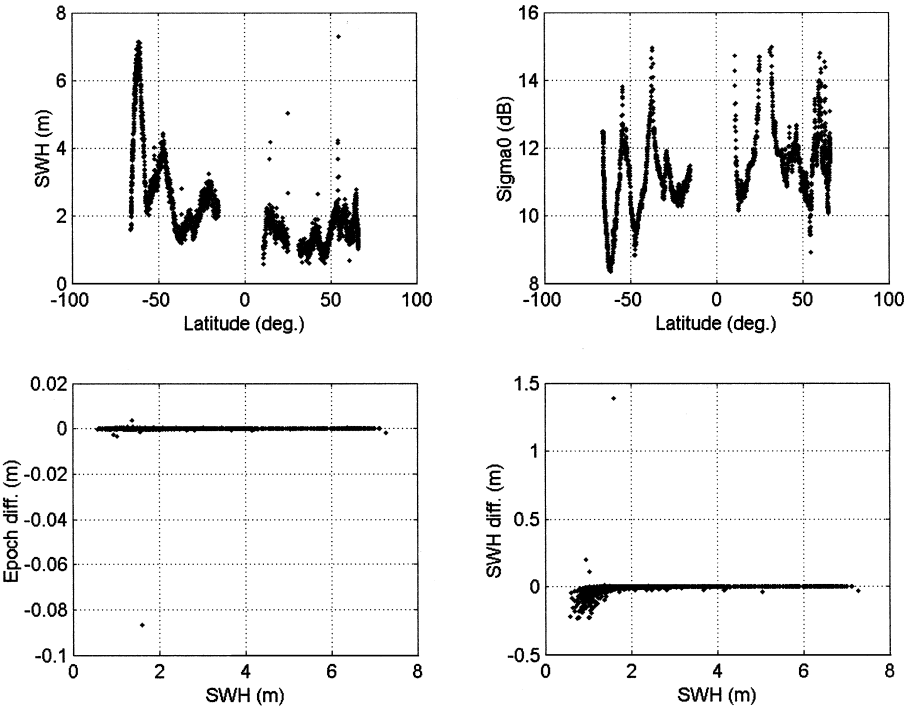

FIGURE 5 Comparison of Poseidon-1 and OZZ ground retracking (pass 13 of cycle 18). Top left, SWH; top right, Sigma0; bottom left, differences of epoch; bottom right, differences of SWH as function of Jason-1 SWH.

The results of these comparisons are respectively shown in Figures 5 and 6 as differences of epoch and differences of SWH versus SWH. The sea-state conditions are shown through the plot of SWH and Sigma0 as function of latitude.

As far as the Poseidon-1/OZZ configurations (Figure 5) are concerned, except for differences of SWH below 1.5 m SWH, the epoch and SWH differences have negligible impact on the data. For SWH below 1.5 m, differences in SWH up to −20 cm can be observed in this example. This is due to the difference in the estimation procedure of the SWH parameter (Sigma C or SWH). Nevertheless, these SWH differences have little impact on the results of the study presented in this article.

Regarding the Jason-1/OZZ configurations (Figure 6), one can see that the samples used have a non negligeable impact. Indeed, while there is no trend as function of SWH, a higher noise than the one observed in the previous comparison does appear. It is difficult to draw a conclusion from this simple example, but as we will see later, the samples used will play a role in explaining some of the differences we will observe.

Once the waveforms have been retracked, the high rate ranges and the 1 Hz SWH can be computed using the equations given in Appendix I.

Noise Level Results and Analysis

Noise Level Computation and Editing Criteria

The high rate Ku-band range noise level is computed through spectral analysis using the raw SSH residuals (Orbit altitude – range – MSS Height) where the mean sea surface (MSS)

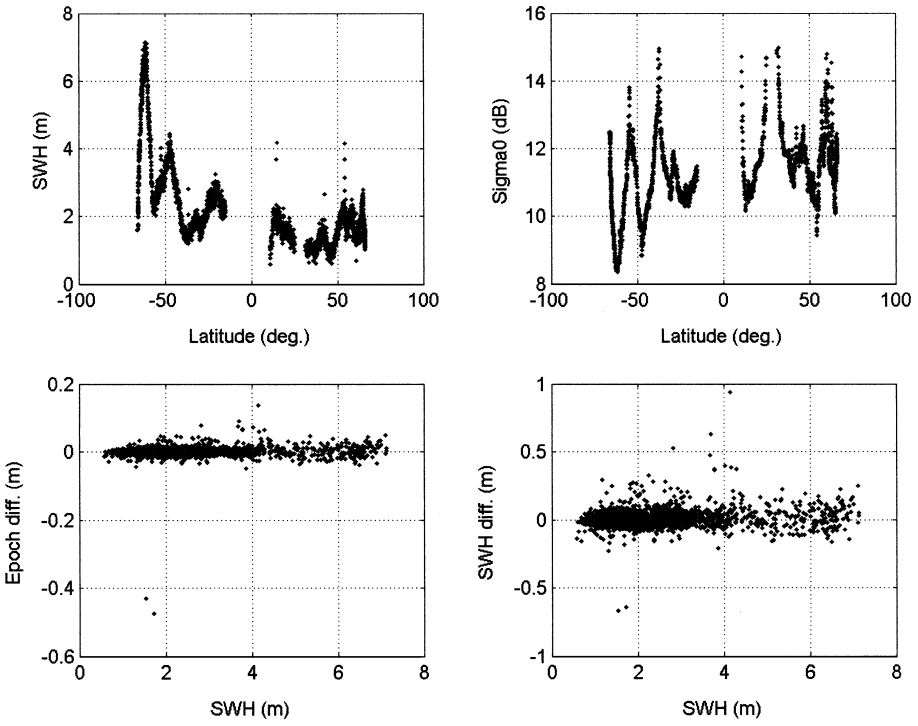

FIGURE 6 Comparison of Jason-1 and OZZ ground retracking (pass 13 of cycle 18). Top left, SWH; top right, Sigma0; bottom left, differences of epoch; bottom right, difference of SWH as function of Jason-1 SWH.

in the user products has been replaced by the CLS 01 MSS from Hernandez et al. (2000) to insure consistency. The periodogram method is used and the procedure is as follows. After editing, data are gathered into continuous segments of 20 s (filling gaps using linear interpolation, only one invalid or missing point allowed). For each segment, the data are fitted by a degree 1 polynomial. Noise is then derived from the residuals. Power spectrum density (PSD) of these residuals is computed and a variance is deduced from the high frequency part of the spectrum.

For each segment, the average value of SWH is also computed and will serve for binning the data per class of SWH (0.25 cm).

The corresponding equations are:

$$\text{Noise (cm)} = \sqrt{\frac{\text{Noise (m}^2\text{/Hz)}^*10^4}{2^*\Delta\tau}}, \tag{8}$$

with

$$\text{Noise (m}^2\text{/Hz)} = \frac{1}{N}\sum_{f_c}^{f_{\max}} \text{PSD}(f), \tag{9}$$

and

$$\text{PSD}(f) = \frac{1}{L}\sum_{l=1}^{L} \frac{\frac{1}{M}\left|\sum_{k=0}^{M-1} x_l(k)w(k)e^{-2\pi jfk}\right|^2}{\frac{1}{M}\sum_{k=0}^{M-1} w^2(k)}, \tag{10}$$

where $\Delta\tau$ is the time sampling (namely 107 ms for TOPEX and about 100 ms for Poseidon-1 and Jason-1), $f_{\max}$ is the highest frequency (about 5 Hz), f_c is the cut-off frequency, N is the number of samples between f_c and $f_{\max}$, x is the high rate input signal, w the weight to be applied on x, L the number of sections, M the number of 1 Hz points in the sections, and f is the frequency.

The editing criteria were chosen to keep as much realistic data as possible in a first stage:

- type of surface: ocean data,
- latitude: between 55°S and 55°N (to avoid sea ice),
- ocean depth: below −1000 m (open ocean),
- SWH: between 0 and 10 m,
- Sigma0: between 8 and 15 dB, and
- Number of high rate valid data: greater than or equal to 9.

In a second stage, editing using statistic indicators on each segment was performed, to keep the segments with stable conditions:

- Standard deviation of SWH: below 0.5 m,
- Standard deviation of Sigma0: below 0.5 dB,
- Standard deviation of SSH residuals: below 0.1 cm, and
- Average of SSH residuals: within ± 1 m.

Example: Results for a Single Pass

As an example, the PSD of the SSH residuals of pass 13 for Poseidon-1 (cycle 361), Jason-1 (cycle 18), and TOPEX (cycle 360) deduced from user products are represented in Figure 7. No binning per SWH class has been performed: the spectra are thus relative to all SWH values found in these passes. In the figures, the abscissa are in Hz and the ordinates are in cm equivalent to noise level.

As one can note, the spectra are quite different. The Poseidon-1 and Jason-1 exhibit a noise floor from 2 Hz to 5 Hz, from which a noise level can be computed using a cut-off frequency of 2 Hz. The TOPEX spectrum, however, shows a signal that continuously drops at these frequencies (slope of 1 cm/Hz, in a 1 Hz to 4.5 Hz range), which actually prevents the computation of a white noise level. Nevertheless, as we are interested in their relative behavior, we will use the same noise computation procedure for all altimeters.

Thus, using a 2 Hz cut-off frequency, the high rate (10 Hz) noise levels are equal to 1.8 cm for TOPEX and about 5.0 cm for Poseidon-1 and Jason-1. The reason for such a difference will be discussed later.

As far as weights w of Equation (10) are concerned, comparative tests have been performed between the simple, averaged, modified, or Welch (using a Hamming window) periodogram methods. To a level of precision of 0.05 cm, and using the noise level computation given above, all these methods yield the same results.

The spectra of the OZZ retracked data along the same tracks are shown in Figure 8. As one can note, little difference from Figure 7 is observed for Poseidon-1 and Jason-1, as they are already retracked in the user products. On the other hand, the TOPEX spectrum exhibits a weaker slope between 1 Hz and 5 Hz (0.5 cm/Hz instead of 1 cm/Hz), and the high frequency level is higher (4.5 cm instead of 1 cm). This allows the display of a "noise floor" as it exists for the other altimeters.

While the noise values for Poseidon-1 and Jason-1 remain the same, about 5 cm, the TOPEX one jumps from 1.8 cm to 5.2 cm, reaching the same noise level as the other altimeters.

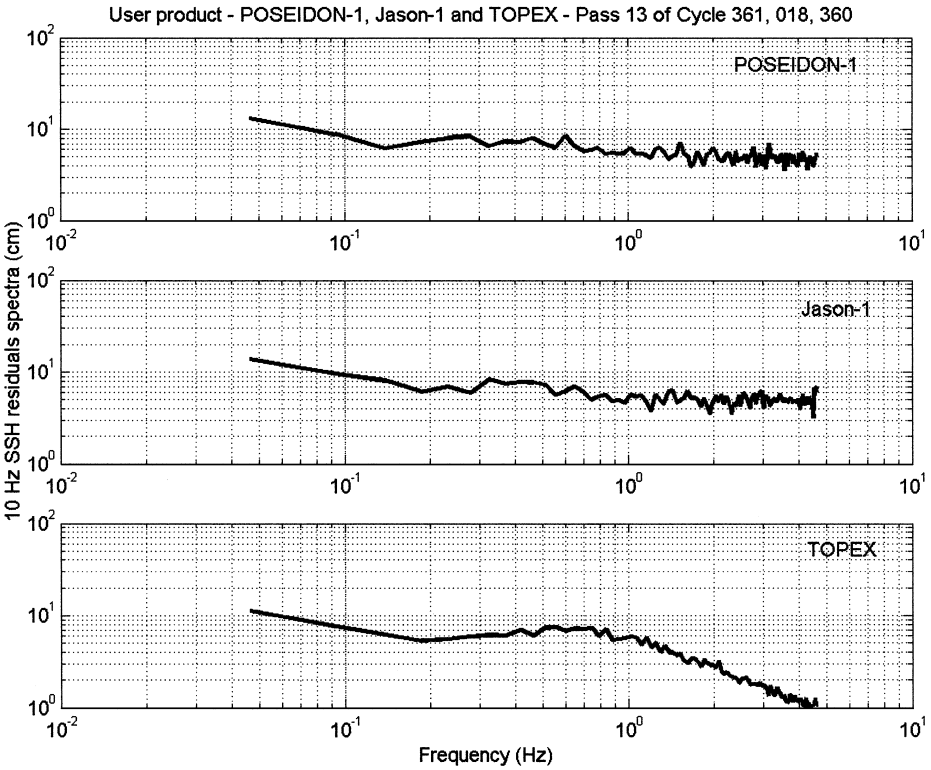

FIGURE 7 Poseidon-1, Jason-1, and TOPEX 10 Hz SSH residual spectra from user product.

The 1 Hz noise level is then obtained by dividing the high rate noise level by the square root of the number of uncorrelated samples. This number is obtained through the correlation analysis of the high rate SSH residuals. The correlation graphs for Poseidon-1, Jason-1, and TOPEX, for user products and for OZZ retracking, are given in Figure 9 as a function of time. The Poseidon-1 correlations from user products and OZZ retracking exhibit a very good stability. If we consider that starting from a threshold of 20% and below, the data are uncorrelated, we can deduce that, out of 10 Hz data, Poseidon-1 has nine uncorrelated points. As expected, results from correlation analysis for Jason-1 are similar to the Poseidon-1 result, and are even better as all the points are below 20%, thus giving 10 uncorrelated points. For TOPEX, the correlations obtained are as expected. Indeed, for an α, β tracker, a correlation of at least two points is expected if no retracking is performed. This is the case as the number of uncorrelated points is eight. Once retracking is applied, the correlation goes down and the number of uncorrelated data is equal to 10, as for Jason-1 altimeter.

In conclusion, when the retracking algorithm is applied to the three data sets (making them consistent in term of processing), all altimeters exhibit the same noise level: 5 cm at 10 Hz and 1.7 cm at 1 Hz.

Noise as a Function of SWH

Binning the data per 0.25 cm classes of SWH gives the opportunity to compute the noise level as a function of SWH. This was performed using the 218 passes that have been processed.

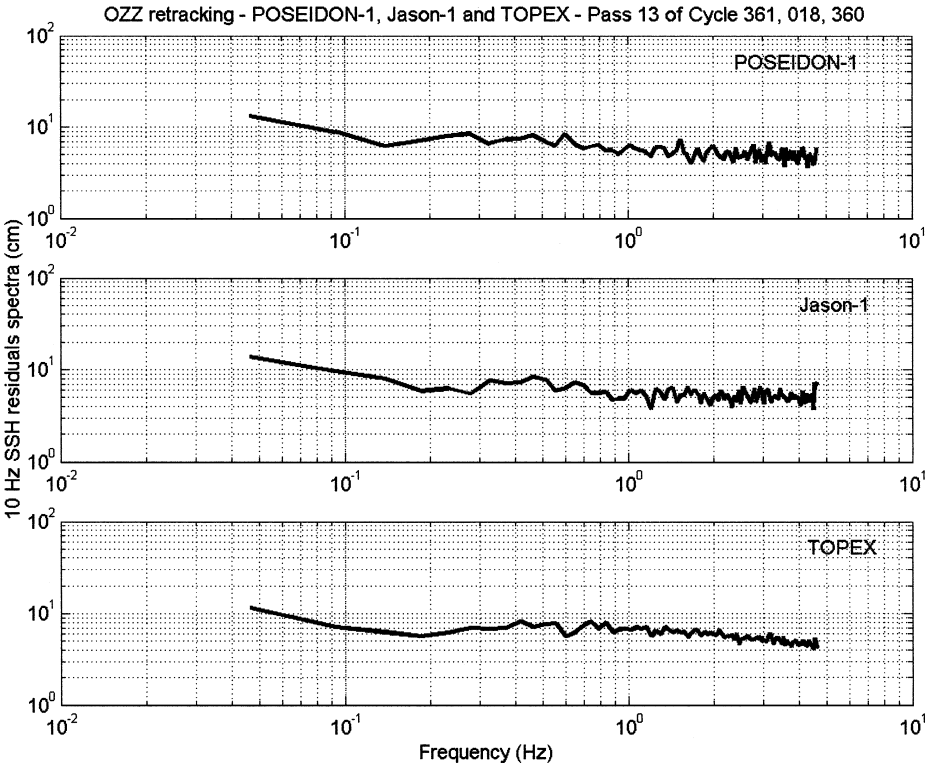

FIGURE 8 Poseidon-, Jason-1, and TOPEX 10 Hz SSH residual spectra from OZZ retracking.

The 10 Hz noise level values are plotted as a function of SWH in Figure 10a for Poseidon-1, Figure 10b for Jason-1, and Figure 10c for TOPEX, for both user products and the coherent OZZ reprocessed data (circle and asterisk). Given the number of data in each class, the results are meaningful only between 1 and 7 m.

For Poseidon-1, the noise levels deduced from the user products and the retracked products are equivalent; they range from 4 cm at 1 m SWH to 7.5 cm at 6 m SWH along a straight line. At a 2 m SWH, the 10 Hz Poseidon-1 noise level is equal to 4.7 cm. The 1 Hz noise level is then equal to 1.6 cm, assuming a number of uncorrelated points equal to nine.

For Jason-1, the noise level deduced from the OZZ retracking is slightly higher than the one deduced from the user product. The fact that the noise versus SWH slope increases from 0.5 cm/m to 0.7 cm/m is due to the number of samples used in the retracking procedures and shall not be related to any SSB effect which does not affect the high frequency part of the range spectrum. Indeed, a test was performed to evaluate the impact of the samples used qualitatively. Using our retracking procedure, passes 7 to 19 of cycle 18 have been retracked with the Jason-1 configuration (using samples 14 to 116). Noise levels as function of SWH were then computed. They are shown in Figure 11 together with the ones issued from OZZ retracking configuration. As it can be seen, the noise levels issued from the Jason-1 configuration are systematically below the OZZ configuration ones, which tends to confirm the assumption that the different samples used are responsible for the trend difference. Investigations on waveforms are currently under way to fully understand this behavior.

Finally, at 2 m SWH the 10 Hz noise level is equal to 5.2 with a number of uncorrelated points equal to 10. Thus, the 1 Hz noise level is equal to 1.6 cm at 2 m SWH.

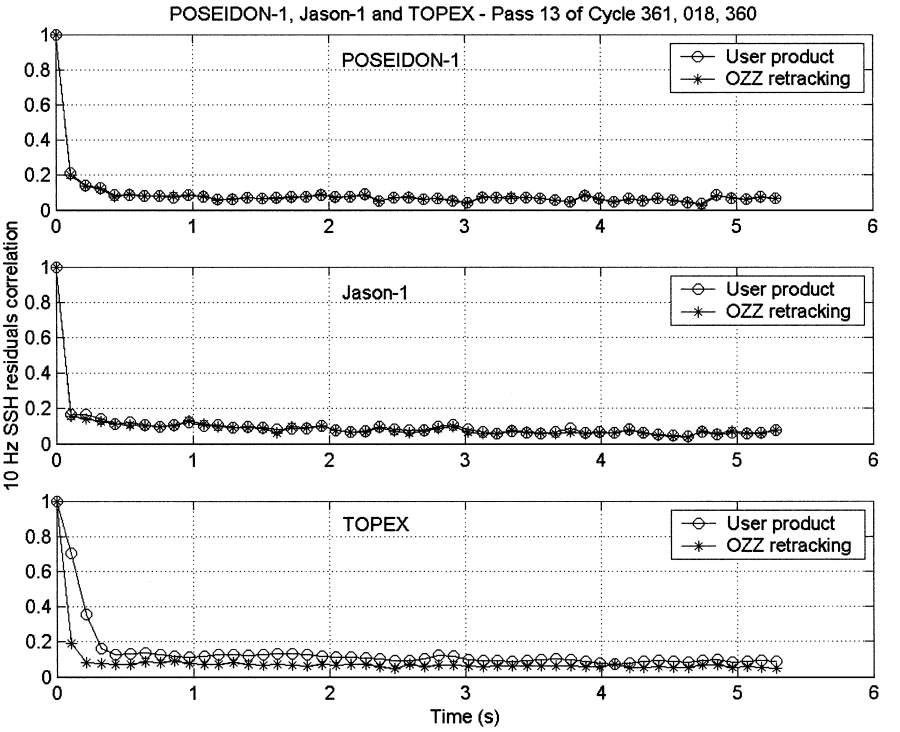

FIGURE 9 User product and OZZ retracking correlation for Poseidon-1, Jason-1, and TOPEX (Pass 013 of cycle 361, 018, and 360).

As far as TOPEX is concerned, in Figure 10c we can distinguish three regions along the SWH parameter: a first region between 1 and 3 m, a second region between 3 and 6 m, and a third region above 6 m. In each region, the behavior of the noise level is the same. For the user product, it starts with a steep increase and then decreases with a smaller slope. For the OZZ retracking data, the noise level shows a linear trend and then at a transition jumps to a higher level. The appearance of these regions is not a surprise and is attributed to the well known "gate index" feature of the TOPEX altimeter and, as we can notice, the retracking smooths the effect of this feature. This was already shown by Rodriguez et al. (1994a).

Back to quantitative considerations of noise level, the 1 Hz noise level is the same as for Poseidon-1 and Jason-1 after OZZ retracking, that is, about 1.6 cm at 2 m SWH, while the one of the user products (recalling that it is not a level of white noise) is very low (between 0.7 cm at 1 m SWH and 1.1 cm at 6 m SWH).

Discussion

As we have seen in the previous two paragraphs, retracking plays an important role in the estimation of the noise level of the altimeter. The fact that the noise level is whitening after retracking is not only valid for the TOPEX altimeter, but also for the Poseidon instruments. Indeed, in Figure 12, the tracker spectra of Poseidon-1 and Jason-1 are plotted together with the TOPEX one (same as the one given in Figure 7c).

As for TOPEX, all spectra exhibit a steep decrease. In the case of the Poseidon-1 and Jason-1 instruments, this decrease starts at frequencies about 0.5–0.6 Hz with a level of 20 cm to reach a level of 4.5 cm at 5 Hz, while for the TOPEX altimeter, it starts at

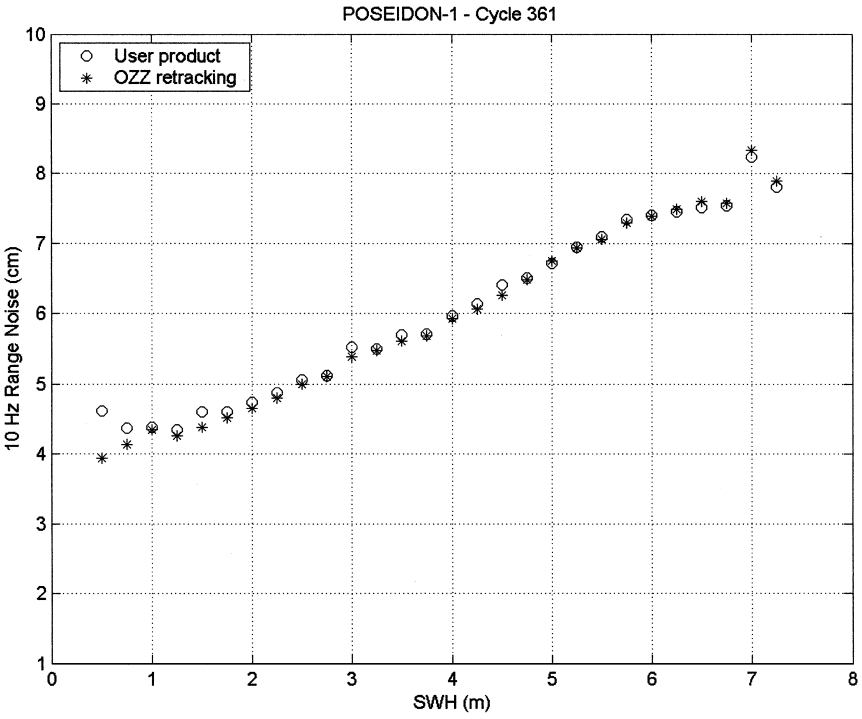

FIGURE 10a Poseidon-1 10 Hz range noise versus SWH.

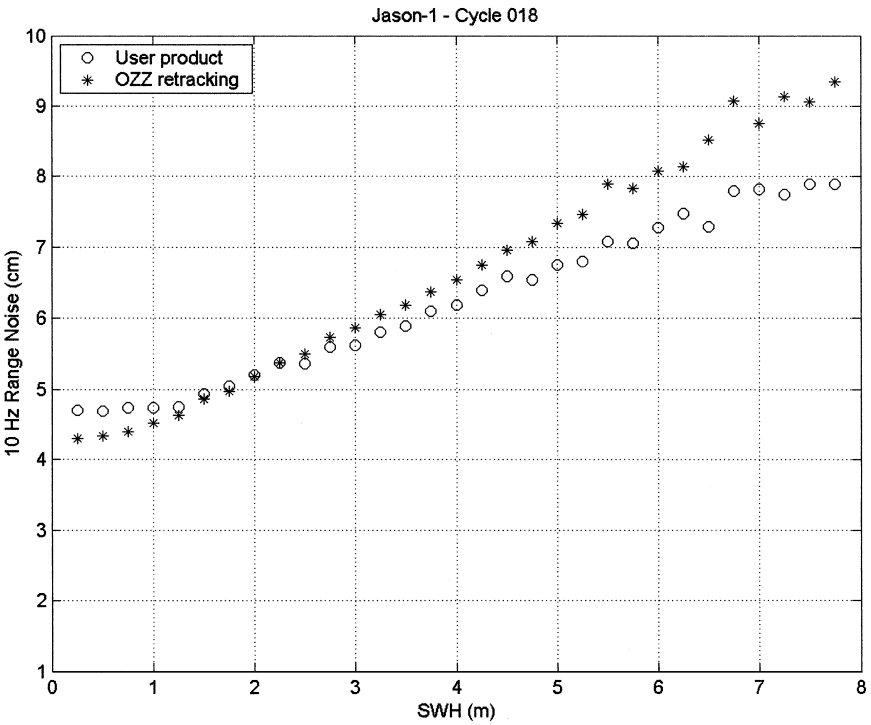

FIGURE 10b Jason-1 10 Hz range noise versus SWH.

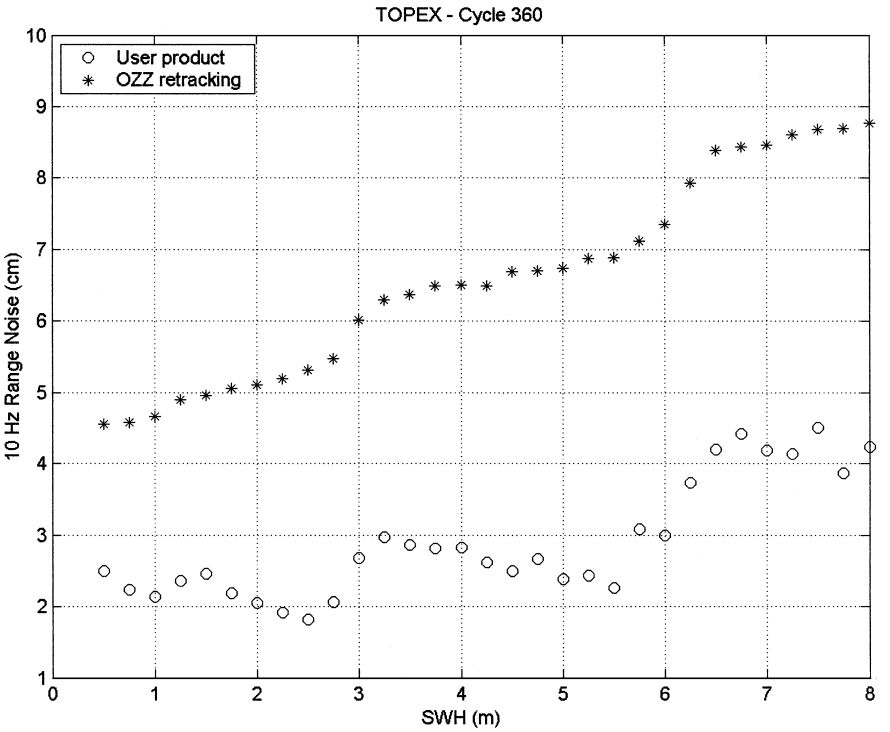

FIGURE 10c TOPEX 10 Hz range noise versus SWH.

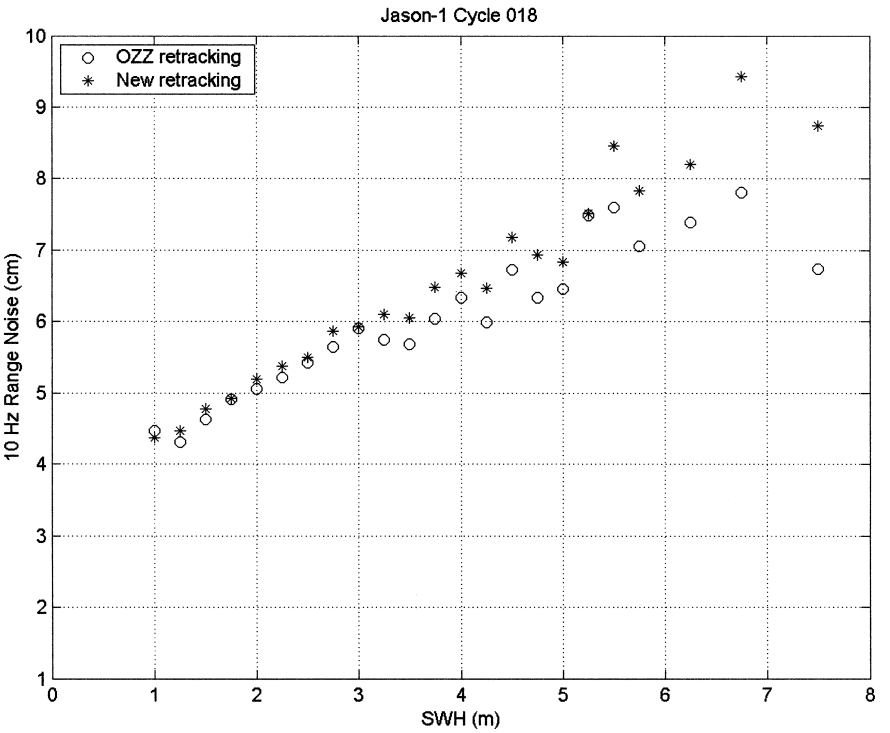

FIGURE 11 Jason-1 range noise versus SWH from new retracking.

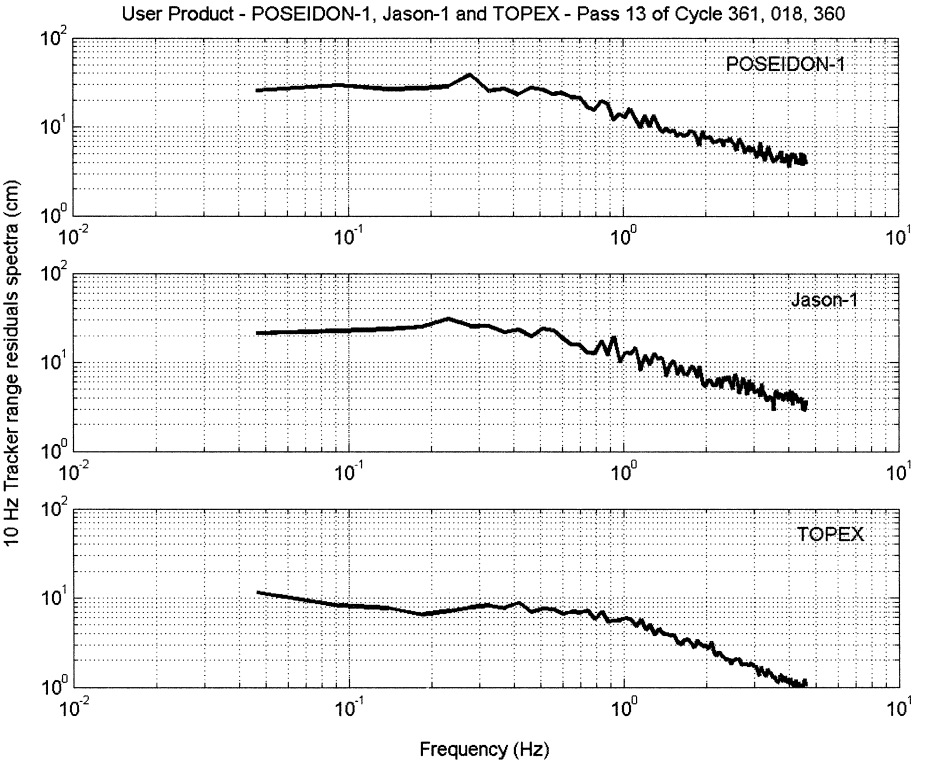

FIGURE 12 Poseidon-1, Jason-1, and TOPEX tracker range spectra.

frequencies about 0.8–0.9 Hz from a level of 6 cm to reach about 1 cm at 5 Hz. The fact that the Poseidon-1, the Jason-1, and the TOPEX spectra start to decrease at different low frequencies is clearly related to the β gain values (see the On-board Tracker section). Also the fact that the energy levels at 5 Hz are different can be related to the noise on the tracker range error (Zanifé, paper to be published).

Also given are the tracker correlations for Poseidon-1 and Jason-1 together with those for TOPEX (Figure 13). As expected, the tracker data are correlated and using the same threshold as before, the number of uncorrelated data is equal to six for Poseidon-1 and Jason-1 altimeters. This number is higher than the one given for TOPEX. This is probably due to the CLn compensation term and the higher β value. Retracking enables the uncorrelation of the data.

The fact that the noise level appears to be the same between Poseidon-1 and Jason-1 instruments and TOPEX after retracking is explained by the minor role of the increase of the PRF above 2000 Hz for SWH less than 6 m (Rodriguez et al. 1994b). This is further confirmed by Quartly et al. (2001). His TOPEX Ku-band waveform study demonstrated that the number of uncorrelated pulses at the tracking point varies from 500 to 1500 over 1 s for SWH ranging between 1 and 5 m. In the same SWH range, the Poseidon-1 value varies from 250 Hz to 1200 Hz, thus giving values close to the TOPEX ones.

Relative SSB

For an altimetric system, the general equation of the 1 Hz SSH relative to the MSS is given by:

$$res\_SSH = Orb - range\_corr - \varepsilon_{environment} - \varepsilon_{SSB} - h_{geophysical} - h_{MSS}, \qquad (12)$$

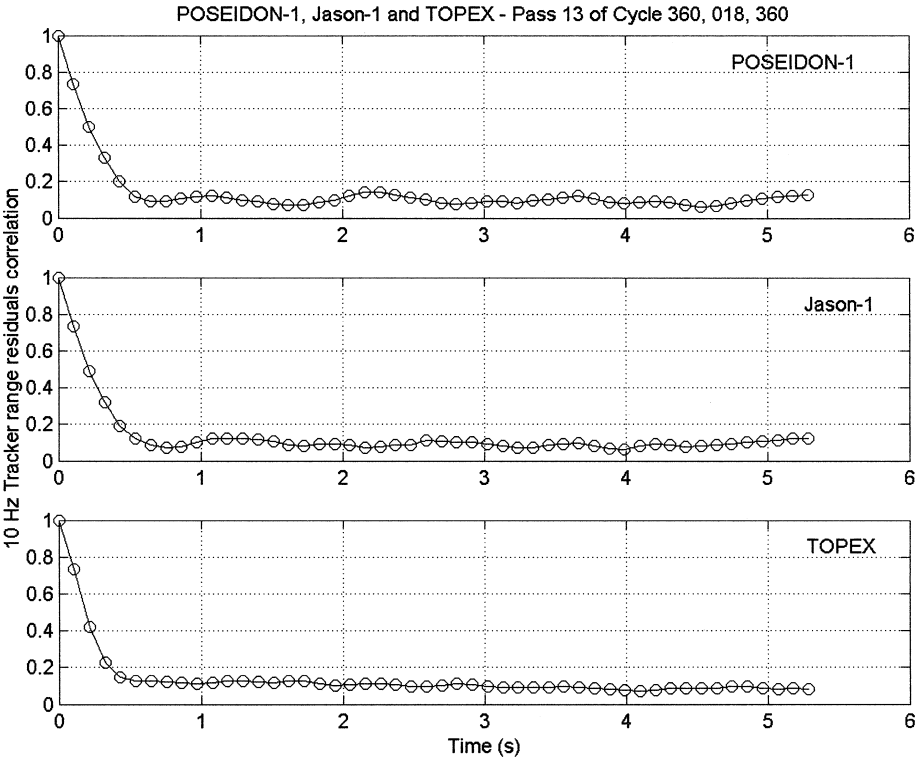

FIGURE 13 Poseidon-1, Jason-1, and TOPEX tracker range correlation.

where *Orb* is the altitude of the satellite above the reference ellipsoid, *range_corr* is the range from the satellite to the sea surface measured by the radar altimeter and corrected for instrumental effects, $\varepsilon_{environment}$ is the sum of the environmental corrections (wet and dry tropospheric and ionospheric corrections), ε_{SSB} is the SSB correction, $h_{geophysical}$ is the sum of the geophysical heights which are essentially tide heights (elastic ocean tide, solid earth tide, nonequilibrium tide, pole tide, and the inverse barometer correction), and h_{MSS} is the MSS height.

For the purposes of this study, and to compensate for the "small" amount of data that have been retracked, collinear differences are used based on the 218 passes that were processed for each altimeter.

Within the period when the TOPEX/Poseidon and Jason-1 satellites were separated by about 72 s, it can be assumed that time separation of measurements is short enough that the environmental corrections and the geophysical heights are the same for both satellites when sensing at the same geographical location. Thus, the $res\_SSH_2 - res\_SSH_1$ difference established for satellites 2 and 1 at the same geographical location is given by:

$$res\_SSH_2 - res\_SSH_1 = (Orb_2 - range\_corr_2 - \varepsilon_{SSB2} - h_{MSS2}) - (Orb_1 - range\_corr_1 - \varepsilon_{SSB1} - h_{MSS1}). \quad (13)$$

Assuming that $res\_SSH_2 - res\_SSH_1$ is null, and expressing SSB as $\varepsilon_{SSB} = \alpha SWH$ (ignoring any wind dependency in a first approximation), it becomes:

$$(Orb_2 - range\_corr_2 - h_{MSS2}) - (Orb_1 - range\_corr_1 - h_{MSS1}) = \alpha_2 SWH_2 - \alpha_1 SWH_1. \quad (14)$$

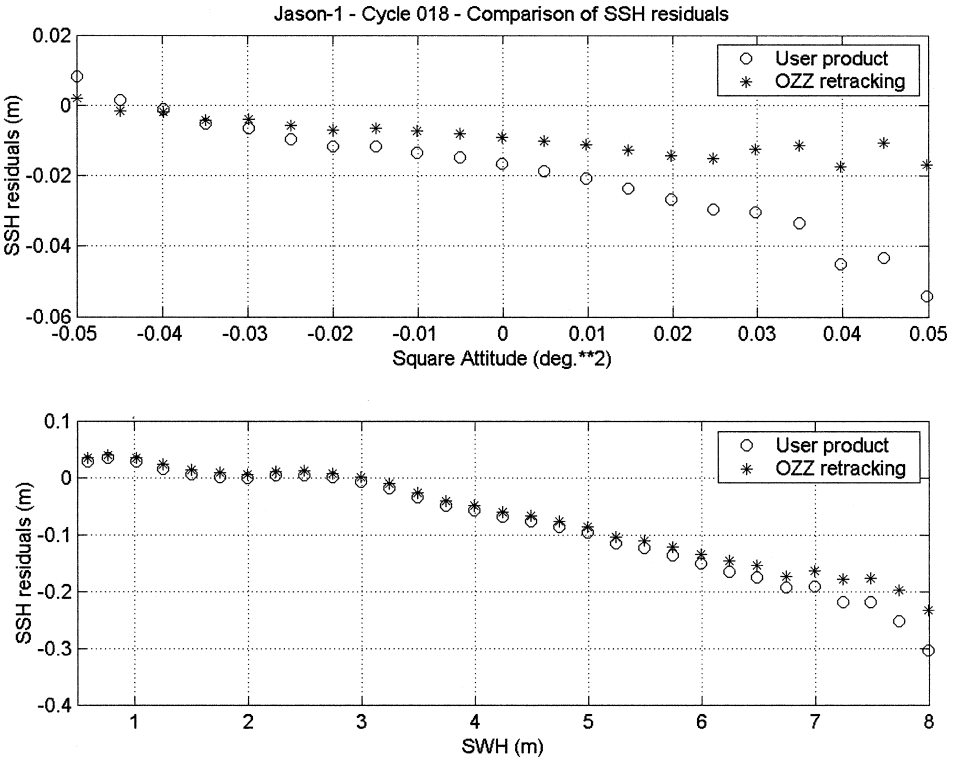

FIGURE 14 Attitude effects on Jason-1 data.

In general the two SWH data sets are not strictly identical; thus, when expressing SWH_2 as function of SWH_1: $SWH_2 = SWH_1 + (SWH_2 - SWH_1) = SWH_1 + \Delta SWH$, the right-hand member of the equation is replaced by $(\alpha_2 - \alpha_1)\, SWH_1 - \alpha_2 \Delta SWH$. As long as ΔSWH is a few percent of SWH_1 , $\alpha_2 \Delta SWH$ can be neglected.

Equation (14) then becomes:

$$(Orb_2 - range\_corr_2 - h_{MSS2}) - (Orb_1 - range\_corr_1 - h_{MSS1}) = (\alpha_2 - \alpha_1) SWH_1, \tag{15}$$

and can be used to derive the relative SSB.

To ease the comparison, Jason-1 will be taken as the reference satellite and will be attributed the index 1. TOPEX and Poseidon-1 will be attributed the index 2.

Attitude Effects

Some investigators (Tournadre, Callahan, personal communications) have reported large attitude effects on Jason-1 data. An example of such effects is shown on Figure 14a, where user products SSH residuals of the 218 passes of cycle 18 are plotted as function of the square of the off nadir angle estimated from the waveforms. Note that the SSH residuals do not account for the ionospheric correction and the electromagnetic bias.

In the square attitude range -0.4 deg.^{2} to $+0.4$ deg.^{2}, the SSH residuals show a dynamic of 4 cm, which is not negligible. To evaluate the impact of this effect in our relative SSB study, the OZZ retracking SSH residuals have been computed over the same passes, and they are also plotted on Figure 14a. In this case, the attitude effect is much smaller than the one observed with the user product as the variation is less than 2 cm over the same

square attitude range. Furthermore, the two SSH residuals have been checked against SWH (Figure 14b), and it is found that both SSH residuals have the same behavior from SWH about 0.5 m to about 7 m SWH. Above 7 m SWH the data are not meaningful due to the small number of points. In conclusion, this effect should have a small impact on our study. This effect can be further reduced with a proper editing of the data.

Poseidon-1/Jason-1 Relative SSB

Estimation from User Products

The SSH residual differences between Poseidon-1 and Jason-1 as a function of Jason-1 SWH (from user products and for the passes listed in the Data Set section) are given in Figure 15c. Also given are the SWH differences as function of Jason-1's SWH and the histogram of the Jason-1's SWH population (Figures 15b and 15a).

As shown by the histogram of the SWH population, only the data between 0.5 m and 7 m are meaningful. As expected, the difference between SWH data set in this range is essentially less than 20 cm, which validates the assumption of neglecting the term $\alpha_2 \Delta SWH$. Detailed analysis of the SWH difference shows four regions in which the SWH difference can be approximated as a straight line with slopes than change signs. Above 5.125 m, the SWH difference seems to remain constant at about 20 cm. For low SWH, below 1.5 m, these features are attributed to the different procedure used to estimate SWH (see sections on Ground Tracking and Data Processing) and to the SWH Look Up table correction of Jason-1. Above 2 m SWH, the observed features are due to the SWH Look Up table correction only.

While the general trend of the user products SSH residuals seems to be a linear function of SWH, a closer analysis shows that the same features as the ones observed for SWH do exist but at slightly different locations. Indeed, the locations are the following: (1) from 0.5 m to 0.75 m; (2) from 0.75 m to 1.25 m; and (3) 1.25 m to 5.25 m. And then above 5.25 m where the points are noisier. Here again, the origins of these features are the same as the ones given for the SWH differences.

As already said, in each of these regions, the SSH residual differences may be modeled as a linear function of SWH_1, and in the region 2 to 5 m, that translates into a relative SSB of the order of 1.1% SWH. As expected, this value is consistent with what is shown in Figure 2. It corresponds on one hand to the normalization correction implemented in Poseidon-1 (refer to the section on Current Knowledge about Noise and SSB and Appendix II), and a contribution of -0.2% SWH that comes from the implementation of a skewness coefficient of 0.1 in the Poseidon-1 ground retracking, and on the other hand, to the Look Up table correction applied on Jason-1 data. This correction behaves like -0.3% SWH between 2 and 6 m SWH.

Estimation from OZZ Retracked Data

The results issued from the OZZ retracking are also shown in Figure 15. For the histogram of the Jason's OZZ retracked SWH population and the differences of retracked SWH, the general comments to be made are the same as those given for the user products: the meaningful population lies between 0.5 m and 7 m, and the maximum absolute SWH difference is less than 10 cm in this SWH range.

Regarding the SWH difference features, one can notice that, except around 1.25 m SWH where a little bump subsists, all these features have disappeared and the curve follows a $-\log$ function. This confirms the assumption made on the origin of these features since, when comparing the OZZ retracked SWH, no corrections are applied.

As shown in Figure 15c, the SSH difference exhibits the same regions as the user product difference but within a 1 cm dynamic compared to the 10 cm dynamic. This means

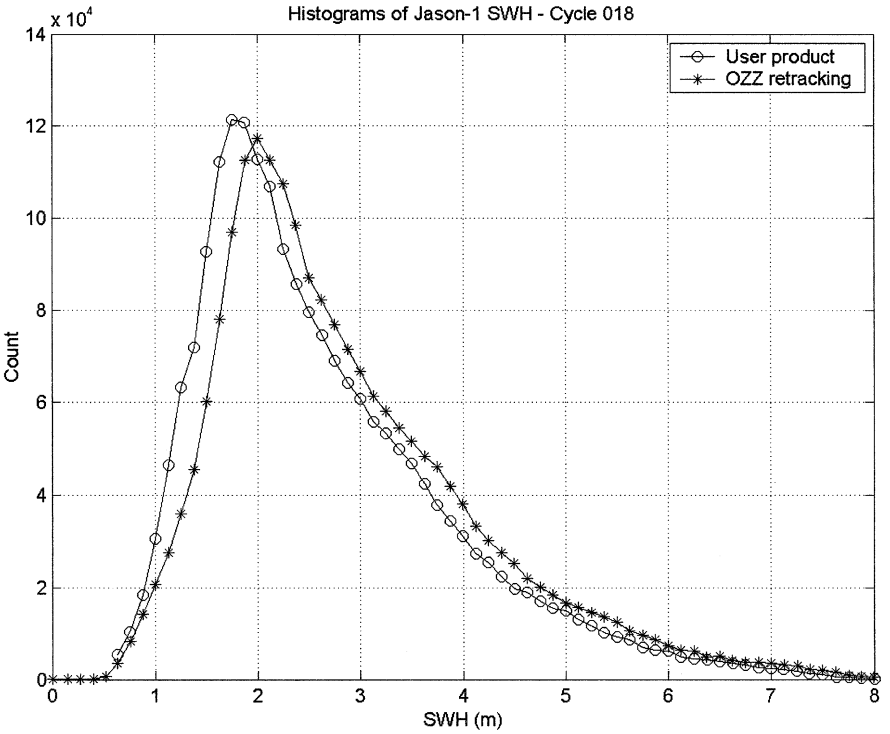

FIGURE 15a Jason-1 SWH histogram comparison.

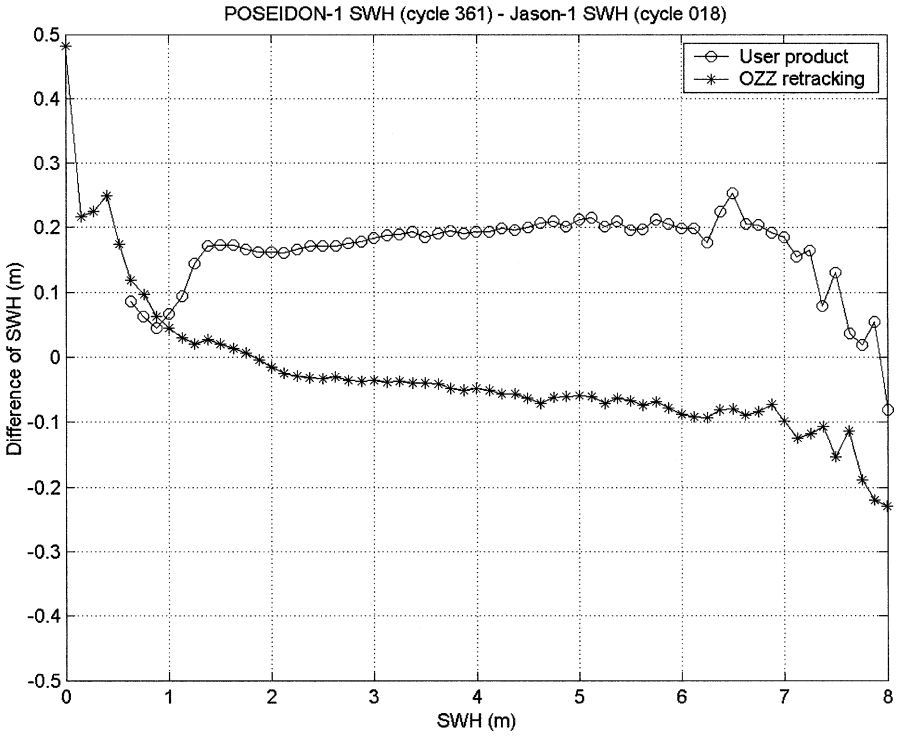

FIGURE 15b Poseidon-1/Jason-1 SWH comparison.

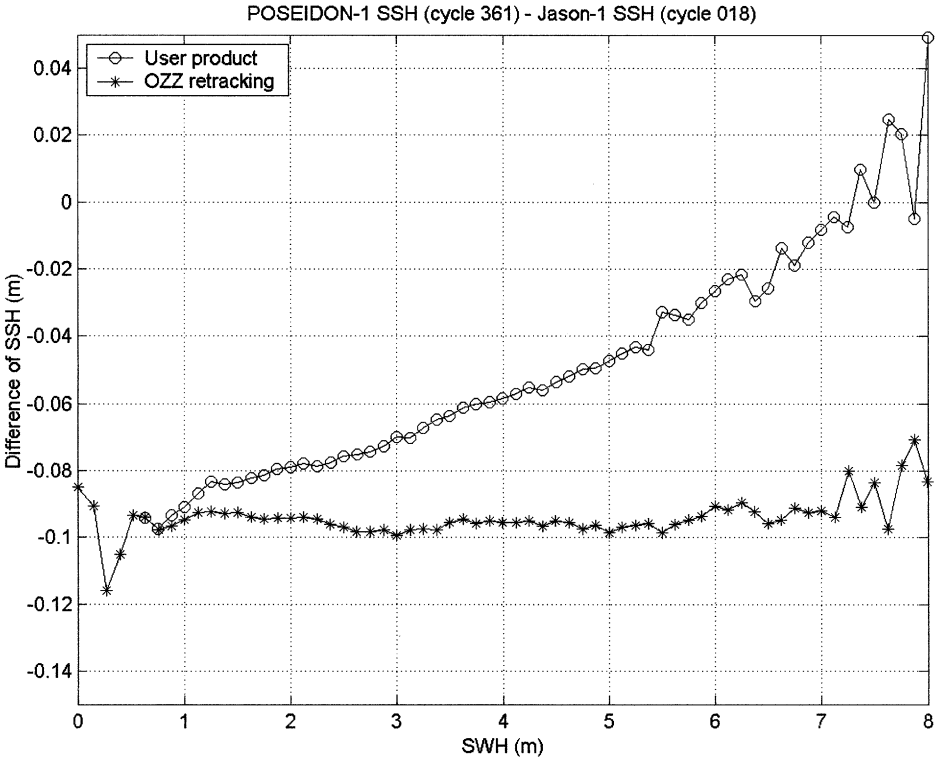

FIGURE 15c Poseidon-1/Jason-1 SSH comparison.

that:

- an additional source to explain the user products SSH differences is to be sought in the waveforms, and
- more importantly, if we look only within the 1 cm dynamic interval, the SSH difference can be approximated as a constant value and thus shows that the relative SSB is equal to zero, meaning that the SSB of both altimeters is the same.

After OZZ retracking, the bias between Poseidon-1 and Jason-1 is about -9.8 cm as shown by the SSH difference between 2 and 5 m SWH. From the user products, if we extrapolate the line given by the SSH difference between 2 and 5 m, the value found at the origin (SWH $= 0$ m) is equal to -11 cm.

TOPEX/Jason Relative SSB

The same analysis has been carried out for the relative SSB between TOPEX and Jason-1, and results are illustrated in Figure 16.

Estimation from User Products

As for the Poseidon-1/Jason-1 case, only the population between 0.5 and 7 m SWH is meaningful. In this interval, the SWH difference is below 30 cm.

One can notice that the SWH difference exhibits several regions as for the Poseidon-1/Jason-1 case. But here they are linked to the gate index features as for the TOPEX noise levels (see Figure 10c). They seem to have the same locations in terms of SWH, which are

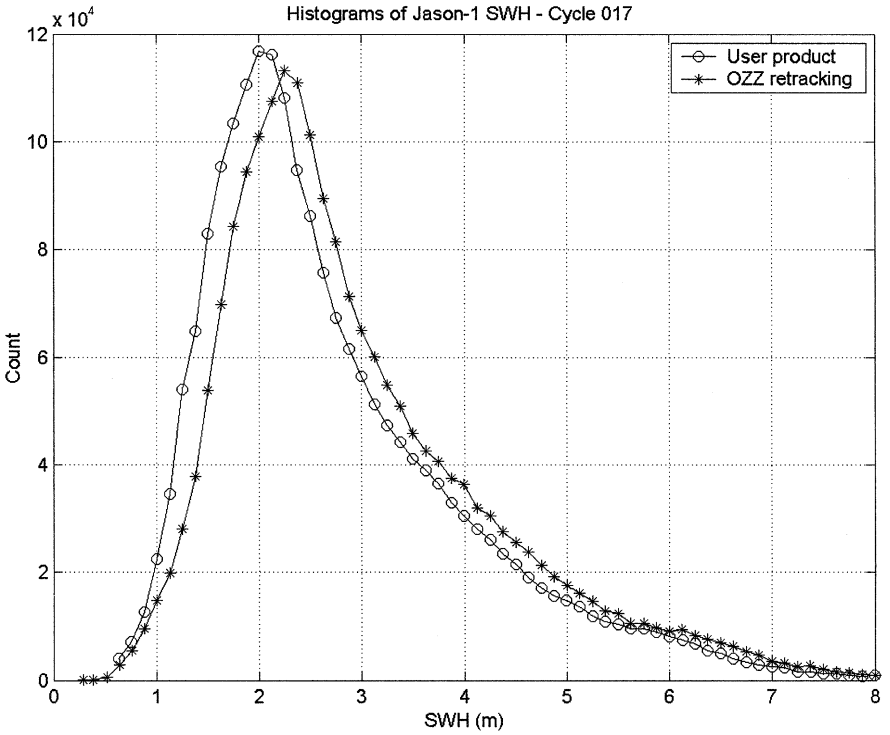

FIGURE 16a Jason-1 SWH histogram comparison.

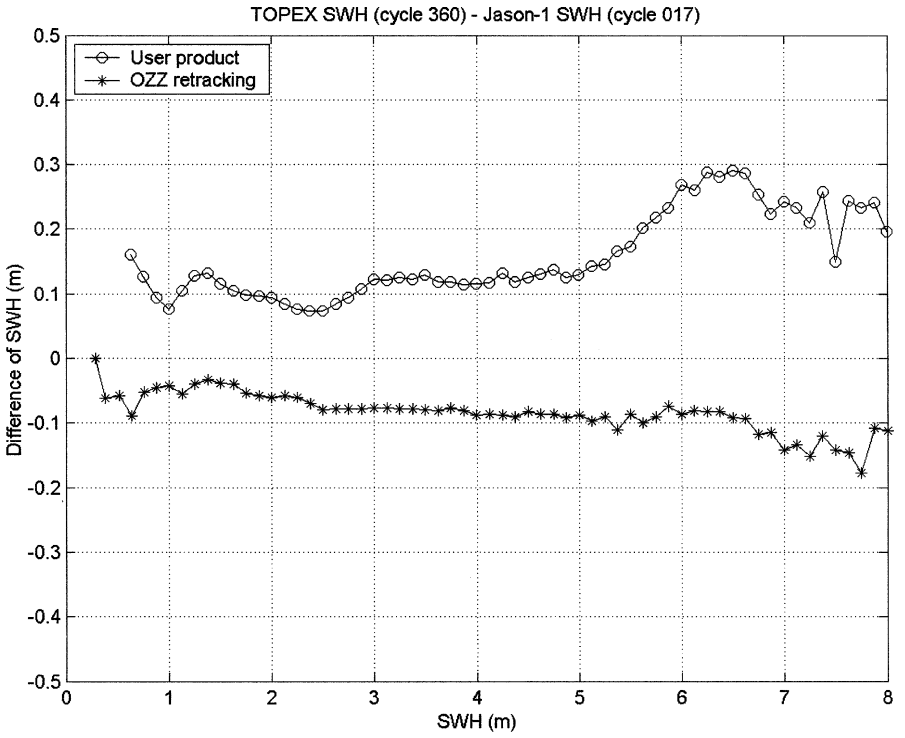

FIGURE 16p TOPEX/Jason-1 SWH comparison.

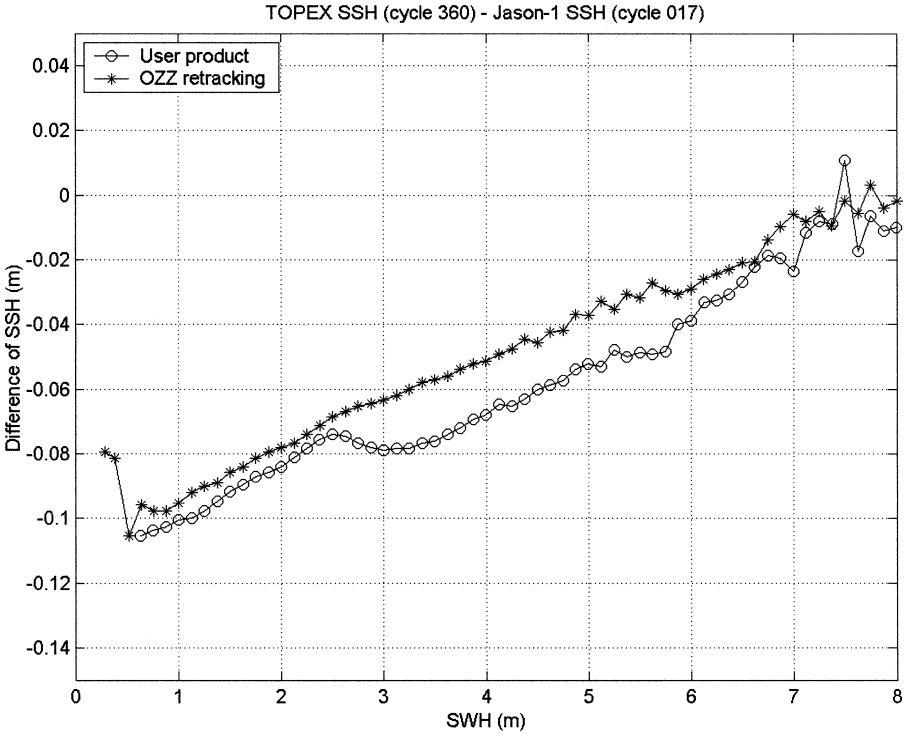

FIGURE 16c TOPEX/Jason-1 SSH comparison.

(1) from 1 to 3 m, (2) from 3 to 6 m, and (3) above 6 m. It should be noticed that between 3 and 6 m SWH the TOPEX gate index effect is balanced by the Look Up table correction. To the level precision of $\pm$ 2 cm, we will consider that the SWH differences are stable between 1 and 5 m and then above 5 m, that they increase by about 15 cm over 1 m, and that they then decrease by about 8 cm.

As far as the TOPEX/Jason-1 relative SSH is concerned, three regions, in which the SSH difference can be modeled as a linear function of SWH clearly appear as for the noise levels. They have the same location: 0.5 to 3 m, 3 to 6 m, and above 6 m. Each of these regions is affected with a subregion of 50 cm wide located before the transition in which the SSH differences are constant. For the first two regions, relative SSB values of 1.7% and 1.5% of SWH have been found. While coherent with the Poseidon-1/Jason-1 figure, this value is higher by about 0.4% SWH. Part of this difference is probably attributed to the variability from one cycle to the other.

Such features (several marked regions) have already been studied by Labroue et al. (2002) using several cycles of TOPEX and Jason-1 data (Jason-1 cycles 3 to 6). In the range 3 to 6 m, the values they have found are lower compared to those we have given above. This again is probably due to the variability of this parameter from cycle to cycle.

We recall that in this article we are not looking for the absolute value of the SSB, but we are interested in comparing the relative SSB using the product on one hand and the relative SSB using the OZZ retracked data on the other hand.

Estimation from OZZ Retracked Data

The results obtained using OZZ retracked data are also displayed in Figure 16. The same comments can be made for the SWH histogram.

For the SWH difference, besides the fact that some bump remains around 1 m and 2.5 m with a very small slope for SWH (3 cm for 1 m), this parameter is very stable around −9.5 cm between 2.5 and 6.5 m SWH. This means that the retracking process has smoothed most of the effect of the gate index. The general trend of this parameter compared to the Poseidon-1/Jason-1 one suggests that the Jason-1 waveforms below 2 m SWH behave more like those of TOPEX than like those of Poseidon-1.

The SSH difference (Figure 16c) in a first approximation aligns itself along a line and does not have the bump as the user product. Nevertheless, a detailed analysis shows that the same three regions can be distinguished as with the user products. And in each of the first two regions, the SSH difference presents SWH slopes very close to the ones obtained from the user products.

Let's recall that retracked data have been obtained using the equations in Appendix I: for TOPEX, the acceleration correction and the SWH/attitude correction (SWH_ATT) have been replaced by the output of the OZZ retracking, and for Jason-1 we have replaced the retracking output of the user products with the one we have computed. This indicates that the retracking process does not cancel the relative SSB. The cause for this relative SSB has thus to be sought somewhere else. This also means that the retracking is actually equivalent to the use of both the acceleration correction and the SWH_ATT term.

Finally, it can be seen that the bias at the origin (SWH = 0 m) is the same as the one given before (about −11.0 cm). It is coherent with the current finding of −13.0 cm (Vincent et al. 2003) which so far has not been explained. A short discussion on relative SSH biases is given in Appendix III.

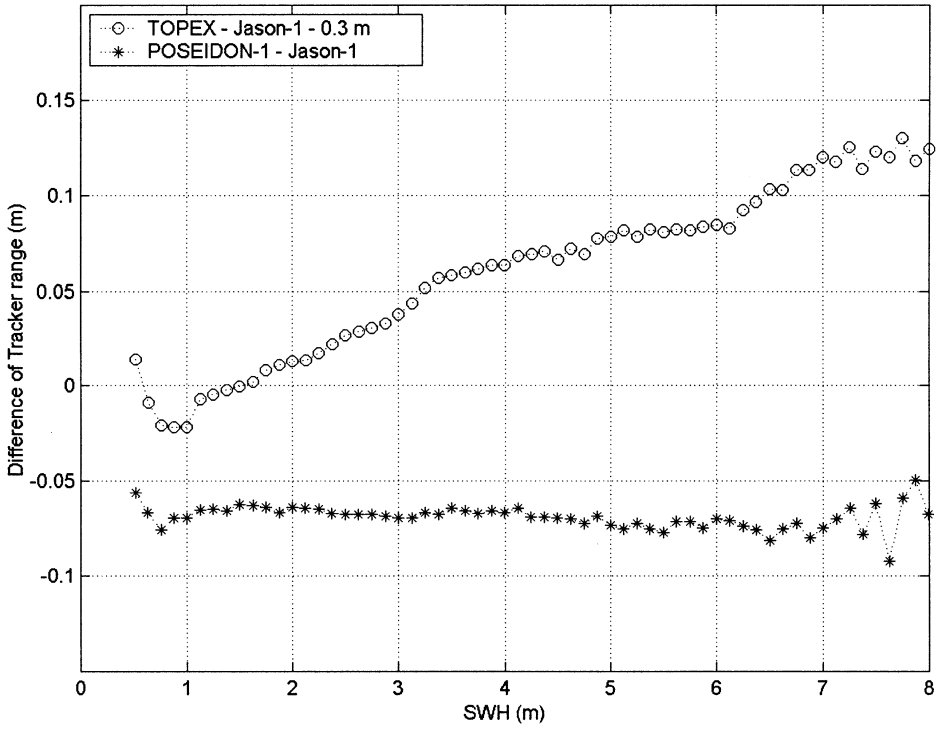

FIGURE 17 TOPEX/Jason-1 and Poseidon-1/Jason-1 Trackers SSH differences.

Relationship between Relative SSB and Different Tracker Algorithms

From the results in the previous section, the relative SSB may come from a different behavior of the on-board trackers. From Figure 17, the difference of Poseidon-1/Jason-1 tracker SSH aligns very closely to a horizontal line, showing a very weak dependency on SWH. For TOPEX/Jason-1, the SSH difference is close to 2% of SWH. Out of this 2% figure, retracking (or the acceleration correction plus the SWH_ATT) removes 0.2 to 0.3% of SWH. We are then left with about 1.7% of SWH due to the different behaviors of the TOPEX and Poseidon instruments, which turns out to be about the value of the first coefficient of the normalization correction on Poseidon-1.

The fact that Poseidon-1 and Jason-1 have the same tracker SSB indicates that both instruments behave the same way. This result was expected as these two instruments are similar and are using the same algorithms. At this point of the study, we are not able to determine what are the contributions of the TOPEX and Jason-1 altimeter in their relative SSB of about 2%.

Other retracking algorithms do exist. They were developed in the frame of the ERS and ENVISAT missions, and by JPL to retrack the TOPEX data. Past internal studies at CLS have shown that all of them, as long as they were used in the same conditions, gave the same answer. Furthermore, recent comparison with the JPL algorithm came to the same conclusions.

Thus the only subsystem that is left to explain the remaining relative SSB is the tracker. Part of it has been explained in this article, but more needs to be done. A detailed simulation of the TOPEX and Jason-1 trackers is envisaged to explain this relative SSB.

Conclusions

In this article we have been looking for the sources of the differences in range noise level and SSB models between the TOPEX and the Poseidon-1/2 radar altimeters. The analysis of the three systems has pointed out three possible sources for explaining such differences: the PRF, the on-board tracker, and the ground retracking.

Comparisons of the three systems have been based on measurements acquired when the TOPEX/Poseidon and Jason-1 satellites were on the same track and when the Poseidon-1 instrument was switched on (cycle 361). All data have been reprocessed using a common ground retracking procedure to generate comparable data sets for all three altimeters.

After ground retracking, range noise levels were computed using spectral analysis. The values found for Poseidon-1 and Jason-1 are coherent with the one derived from the user products, in which a ground retracking algorithm very close to the one used in this article is applied. For standard conditions (2 m SWH), the noise level is equal to 5 cm for 10 Hz data, which converts into 1.6 cm for 1 Hz data. Retracking TOPEX data whitens the high frequency component of the spectra and allows decorrelation of the data. The noise level values found for TOPEX are equivalent to those of Poseidon-1 and Jason-1. This confirms that, for SWH ranging between 1 m and 6 m, high PRFs as for TOPEX do not play a significant role after application of the retracking.

Validating TOPEX retracked data also helped in demonstrating that the acceleration correction and the so-called SWH_Att correction found in the TOPEX standard user products have the same role as retracking.

Coming back to tracker data, we could show that the relative SSB lies in the difference between TOPEX and Poseidon-1, Jason-1 tracker algorithms. Further detailed studies of the TOPEX and Jason tracking loops are needed to identify the exact source of the relative SSB.

Explaining the relative SSH biases between all altimeter systems is more tricky. However, results displayed in this article tend to favor the tracker systems as possible candidates for explaining these biases.

This study has been performed with IGDR/SGDR products. It is also planned to perform tests with the new GDR/SGDR products which have been improved compared to the IGDR/SGDR products.

References

AVISO/Altimetry. 1996. *AVISO User handbook—Merged TOPEX/Poseidon Products (GDR-Ms)*, Tech. Note, AVI-NT-02-101-CN, Issue 3.0, Ed. by CNES.

Brown, G. S. 1977. The Average impulse response of a rough surface and its application. *IEEE Transactions on Antenna and Propagation* AP.25(1):67–74.

Carayon, G., N. Steunou, J.-L. Courrière, and P. Thibaut. 2003. Poseidon 2 radar altimeter design and results of in flight performances. *Mar. Geod*. This issue.

Chelton, D. B., E. J. Walsh, and J. L. MacArthur. 1989. Pulse compression and sea level tracking in satellite altimetry. *J. Atmos. and Oceanic Tech.* 6:407–438.

Chelton, D. B., J. C. Ries, B. J. Haines, L.-L. Fu, and P. S. Callahan. 2001. Satellite altimetry and earth sciences, Chapter 1. pp. 1–133. In *Satellite altimetry*. San Diego, CA: Academic Press.

Dorandeu, J., M. H. Delaunay, F. Mertz, and J. Stum. 2001. AVISO/CALVAL Yearly Report: Eight years of TOPEX/Poseidon data. Tech. Note, SMM-NT-EA-12962-CN, Issue 1.0, Ed. by CNES.

Dorandeu, J., P. Thibaut, O. Z. Zanifé, Y. Faugere, G. Dibarboure, G. Carayon, N. Steunou, and P. Vincent. 2002. Poseidon-1, Poseidon-2 and TOPEX noise analysis. Presentation at the New Orleans SWT, October 21–23, 2002.

Dumont, J.-P. 1985. Estimation optimale des paramètres altimétriques des signaux radar Poseidon. PhD Thesis from Institut National Polytechnique de Toulouse.

Dumont, J. P., O. Z. Zanifé, P. Thibaut, P. Mambert, B. Soussi, S. Labroue, S. Gallocher, N. Geiger, J. C. Brun, M. N. Loaec, P. Vincent, T. Guinle, and N. Picot. 2001. CMA altimeter multi-mission center—Production processing. Jason-1/TOPEX/Poseidon Science Working Team Meeting, Biarritz, France.

Escudier, P., G. Kunstmann, F. Parisot, R. Boain, T. Lafon, P. Hoze, and S. Kaki. 2000. Jason system overview and status. *AVISO Newsletter* 7:9–15.

Fu, L.-L., E. J. Christensen, C. A. Yamarone Jr., M. Lefebvre, Y. Ménard, M. Dorrer, and P. Escudier. 1994. TOPEX/Poseidon mission overview. *J. Geophys. Res.* 99(C12):24369–24381.

Gaspar, P., and J. P. Flourens. 1998. Estimating the sea state bias in radar altimeters measurements of sea level: Results from a non parametric method. *J. Geophys. Res.* 103:15803–15814.

Gaspar, P., S. Labroue, F. Ogor, G. Laffite, L. Marchal, and M. Rafanel. 2002. Improving nonparametric estimates of the sea state bias in radar altimeter measurements of sea level. *J. of Atmos. and Oceanic Tech.* 19:1690–1707.

Gaspar, P., F. Ogor, P. Y. Le Traon, and O. Z. Zanifé. 1994. Estimating the sea state bias of the TOPEX and Poseidon altimeters from crossovers differences. *J. Geophys. Res.* 99(C12):24981–24994.

Hayne, G. S. 1980. Radar altimeter mean return waveform from near-normal-incidence ocean surface scattering. *IEEE Transactions on Antenna and Propagation* AP.28(5):687–692.

Hayne, G. S., D. W. Hancock III, and C. L. Purdy. 1994. The corrections for significant wave height and attitude effects in the TOPEX radar altimeter. *J. Geophys. Res.* 99(C12):24941–24955.

Hernandez, F., and P. Schaeffer. 2000. Altimetric mean sea surfaces and gravity anomaly maps intercomparisons. AVI-NT-011-5242-CLS. St Agne, France: CLS Ramonville.

Labroue, S., P. Vincent, and P. Gapar. 2002. TOPEX and Jason-1 sea state bias estimation. Post-SWT Jason-1 meeting, AGU, San Francisco, December 7, 2002.

Marth, P. C., J. R. Jensen, C. C. Kilgus, J. A. Pershy, J. L. MacArthur, D. W. Hancock, G. S. Hayne, C. L. Purdy, L. C. Rossi, and C. J. Koblinsky. 1993. Prelaunch performance of the NASA altimeter for the TOPEX/Poseidon project. *IEEE Transactions on Geoscience and Remote Sensing*. 31(2):315–332.

Ménard, Y., L. L. Fu, P. Escudier, B. Haines, G. Kunstmann, F. Parisot, J. Perbos, P. Vincent, and S. Desai. 2003. The Jason-1 Mission. *Mari. Geod.* This issue.

Perbos, J., P. Escudier, F. Parisot, G. Zaouche, P. Vincent, Y. Ménard, F. Manon, G. Kunstmann, D. Royer, and L. L. Fu. 2003. Jason-1: Assesment of the system performances. *Mar. Geod.* This issue.

Quartly, G. D., M. A. Srokosz, and A. C. McMillan. 2001. Analyzing altimeter artefacts: Statiscal properties of ocean waveforms. *J. of Atmos. and Oceanic Tech.* 18:2074–2091.

Raizonville, P., B. Cugny, O. Z. Zanifé, Y. Jaulhac, and J. Richard. 1991. Poseidon radar altimeter flight model design and tests results. *Proceedings of IGARSS'91* pp. 1773–1778.

Rodrìguez, E. 1988. Altimetry for non-gaussian oceans: Height biases and estimation of parameters. *J. Geophys. Res.* 93(C11):14107–14120.

Rodrìguez, E., and J. M. Martin. 1994a. Correlation properties of ocean altimeter returns. *IEEE Transactions on Geoscience and Remote Sensing*. 32(3):553–561.

Rodrìguez, E., and J. M. Martin. 1994b. Assesment of the TOPEX altimeter performance using waveform retracking. *J. Geophys. Res.* 99(C12):24957–24969.

Tran, N., D. W. Hancock III, G. S. Hayne, D. W. Lockwood, D. Vandemark, M. L. Driscoll, and R. V. Sailor. 2002. Assessment of the cycle-to-cycle noise level of the geosat follow-on, TOPEX, and poseidon altimeters. *J. of Atmos. and Oceanic Tech.* 19:2095–2107.

Vincent P., S. D. Desai, J. Dorandeu, M. Ablain, B. Soussi, P. S. Callahan, and B. J. Haines. 2003. Jason-1 geophysical performance evaluation. *Mar. Geod.* This issue.

Walsh, E. J. 1982. Pulse-to-pulse correlation in satellite radar altimeters. *Radio Science* 17(4):786–800.

Zanifé O. Z., P. Thibaut, P. Vincent, B. Bonhoure, E. Thouvenot, J. Dorandeu, P. Y. Le Traon, N. Picot, P. Escudier, B. Cugny, P. Raizonville, and M. Dorrer. 2001. Performances of the POSEIDON-1 radar altimeter. *Proceedings of IGARSS*' 2001, July 9–13, 2001.

Zieger, A. R., D. W. Hancock, G. S. Hayne, and C. L. Purdy. 1991. NASA radar altimeter for the TOPEX/Poseidon project. *Proceedings of the IEEE*. 79(6):810–826.

Appendix I

Reconstruction Equations

This appendix gives the equations to be used to reconstruct the SWH and the range parameters after applying a retracking. In the following paragraphs, "*trk*" stands for tracker while "*rtk*" stands for retracking. The latter is used as suffices for the operational ground retracking and as exponents for the retracking used in this study.

SWH Reconstruction

The SWH in the user products are given by the following equations:

TOPEX

$$SWH_{1\,Hz} = SWH\_trk_{1\,Hz} + SWH\_Att\_corr + Cal\_corr, \qquad (1A1a)$$

where $SWH\_trk_{1\,Hz}$ is the average of the high rate SWH estimates issued from the onboard tracker, *SWH_Att_corr* is the Pointing Angle/Sea State correction, and *Cal_corr* is the calibration correction. Actually, in the ground processing, the *Cal_corr* parameter is set to 0.

Poseidon-1

$$SWH_{1\,Hz} = SWH\_rtk_{1\,Hz} + Att\_corr + LookUp\_corr + Syst\_bias, \qquad (1A1b)$$

where $SWH\_rtk_{1\,Hz}$ is the average of the high rate SWH estimates issued from the ground retracking, *Att_corr* is the attitude correction, *LookUp_corr* is the correction computed from the Look Up Table, and *Syst_bias* is the system bias. Actually, in the ground processing, the *LookUp_Table_corr* and the *Syst_bias* parameters are set to 0.

Jason-1

$$SWH_{1\,Hz} = \frac{c}{2} 4\sqrt{SigmaC\_rtk^2_{1\,Hz} - SigmaP^2} + LookUp\_corr + Syst\_bias, \quad \text{(1A1c)}$$

where c is the speed of the light, $SigmaC\_rtk_{1\,Hz}$ is the average of the high rate of the Sigma Composite issued from the ground retracking, *SigmaP* is the width of the Point Target Response, *LookUp_corr* is the correction computed from the Look Up Table, and *Syst_bias* is the system bias. Actually, in the ground processing, the *Syst_bias* parameter is set to 0.

After OZZ retracking, the 1 Hz rate $SWH^{rtk}_{1\,Hz}$ is given by:

$$SWH^{rtk}_{1\,Hz} = Average\ over\ 1\ Hz\ of \left\{ \frac{c}{2} 4\sqrt{SigmaC^{rtk^2}_{10\,Hz} - SigmaP^2} \right\}, \quad \text{(1A2)}$$

where $SigmaC^{rtk}_{10\,Hz}$ is the high rate Sigma Composite issued from the OZZ retracking. This equation is used for the three altimeter data sets.

TOPEX and Poseidon-1 Range Reconstruction

For the range the process is slightly more complicated, as we have to add the output of the tracker to the output of the retracking and to take care of the corrections which have been applied on the range.

TOPEX

The range in the MGDR product is obtained through:

$$alt_{10\,Hz} = alt\_trk\_raw_{10\,Hz} + Sum\_instr\_corr, \quad \text{(1A3)}$$

with

$$Sum\_instr\_corr = SWH\_Att\_corr + Acc\_corr + Doppler\_corr + Track\_corr + USO\_corr + Cal\_corr + COG\_corr, \quad \text{(1A4)}$$

where $alt\_trk\_raw_{10\,Hz}$ is the 10 Hz on-board tracker range (obtained from the 20 Hz data by averaging them two by two), *Sum_instr_corr* is the 1 Hz sum of the instrumental correction which includes the SWH and Attitude correction (*SWH_Att_corr*), the acceleration correction (*Acc_corr*), the Doppler correction (*Doppler_corr*), the Tracker mode correction (*Track_corr*), the Ultra Stable Oscillator correction (*USO_corr*), the Internal calibration correction (*Cal_corr*), and the Center of gravity correction (*COG_corr*).

When considering retracking, the $epoch^{rtk}_{10\,Hz}$ parameter takes care of the *SWH_Att_corr* and the *Acc_corr* parameters. Thus after applying OZZ retracking, the range can be written:

$$alt^{rtk}_{10\,Hz} = alt_{10\,Hz} - SWH\_Att\_corr - Acc\_corr + epoch^{rtk}_{10\,Hz}. \quad \text{(1A5)}$$

The *SWH_Att_corr* is provided in the TOPEX product; however, the acceleration correction is not. It has been recomputed using the same algorithm as in the TOPEX ground segment.

Poseidon-1

As for TOPEX, the range provided in the MGDR product is given by:

$$alt_{10\,Hz} = alt\_trk\_USO_{10\,Hz} + epoch\_rtk_{10\,Hz} + Sum\_instr\_corr, \tag{1A6}$$

with

$$Sum\_instr\_corr = Att\_corr + Doppler\_corr + LookUp\_corr + Norm\_corr + Cal\_corr + COG\_corr + Syst\_bias, \tag{1A7}$$

where $alt\_trk\_USO_{10\,Hz}$ is the 10 Hz on-board tracker range (obtained from the 20 Hz data by averaging them two by two) corrected for the USO effect, $epoch\_rtk_{10\,Hz}$ is the estimate of the epoch from the ground retracking (obtained from the 20 Hz data by averaging them two by two), *Att_corr* is the off nadir angle correction, *LookUp_corr* is the correction computed from the Look Up Tables, *Norm_corr* is the normalization correction (see Appendix II), *Syst_bias* is the system bias, and the other parameters have the same meaning as the ones given in the previous paragraph. In the case of Poseidon-1, the *LookUp_corr* parameter and the *Syst_bias* parameter are set to zero.

Since all these parameters are provided through the MEGA files, it is an easy task to compute the precise range $alt^{rtk}_{10\,Hz}$ derived from the OZZ retracking procedure. It can be done through an equation similar to Equation (1A6):

$$alt^{rtk}_{10\,Hz} = alt\_trk\_USO_{10\,Hz} + epoch^{rtk}_{10\,Hz} + Sum\_instr\_corr - Norm\_corr, \tag{1A8a}$$

or by replacing the epoch retracked by the Poseidon-1 algorithm:

$$alt^{rtk}_{10\,Hz} = alt_{10\,Hz} - epoch\_rtk_{10\,Hz} + epoch^{rtk}_{10\,Hz} - Norm\_corr. \tag{1A8b}$$

Jason-1 Range Reconstruction Associated with GDR

The 20 Hz ranges provided in the GDR to be delivered to users are given by Equation (1A6) as for Poseidon-1 but at 20 Hz rate with:

$$Sum\_instr\_corr = Doppler\_corr + LookUp\_corr + USO\_corr + Cal\_corr + COG\_corr + Syst\_bias. \tag{1A9}$$

Note the parameter *Syst_bias* in the sum of the instrumental corrections is set to 0.

Thus after applying OZZ retracking, the range may be retrieved using an equation similar to Equation (1A8a):

$$alt^{rtk}_{10\,Hz} = alt\_trk_{10\,Hz} + epoch^{rtk}_{10\,Hz} - LookUp\_corr, \tag{1A10}$$

where $alt\_trk_{10\,Hz}$ is the two by two average of the high rate on-board tracker range corrected for all instrumental corrections and is provided in the SGDR product, *LookUp_corr* is provided through the SGDR product.

An equation similar to Equation (1A8b) can also be used:

$$alt^{rtk}_{10\,Hz} = alt_{10\,Hz} - epoch\_rtk_{10\,Hz} + epoch^{rtk}_{10\,Hz} - LookUp\_corr, \tag{1A11}$$

with

$$alt_{10\,Hz} = alt_{1\,Hz} + \Delta alt_{10\,Hz}, \tag{1A12a}$$

and

$$epoch\_rtk_{10\,Hz} = alt_{10\,Hz} - alt\_trk_{10\,Hz}, \tag{1A12b}$$

where $alt_{1\,Hz}$ is the 1 Hz range of the GDR product and $\Delta alt_{10\,Hz}$ is the two by two average of the 20 Hz range differences provided in the GDR product.

Jason-1 Range Reconstruction for Data of the Verification Phase

During the Jason verification phase, the Jason Science software was subject to improvements to take into account elements raised by the investigators. During this phase, SGDR products were associated with the IGDR products available to the science working team. This article is derived from the analysis of the SGDR products computed during this phase. It was then important to derive the equations associated with the products as they were defined at that time.

Thus, after applying retracking, the range can be reconstructed according to Equations (1A10), (1A11), and (1A12). In the following two paragraphs, equations are given to derive the parameters that appear in these equations.

Equations for Cycle 17 and 18 (CMA Version 5.04_5 or Earlier)

The parameter $alt\_trk_{10\,Hz}$ in Equation (1A10) has a different definition from that of the GDR product. In the CMA version used to generate Jason-1 cycle 17 and 18, it is defined as the two by two average of the high rate on-board tracker ranges corrected for the USO correction only. Thus, Equation (1A9) becomes:

$$alt^{rtk}_{10\,Hz} = alt\_trk_{10\,Hz} + Sum\_instr\_corr - USO\_corr + epoch^{rtk}_{10\,Hz} - LookUp\_corr. \tag{1A13}$$

The parameters *Sum_instr_corr* and *USO_corr* are, respectively, provided through the IGDR and the SGDR product; however, the *LookUp_corr* is not. Nevertheless, it can be computed using the following equation:

$$LookUp\_corr = Sum\_instr\_corr - USO\_corr - Doppler\_corr - COG\_corr - Cal\_corr, \tag{1A14}$$

and finally when using this equation, Equation (1A13) becomes:

$$alt^{rtk}_{10\,Hz} = alt\_trk_{10\,Hz} + epoch\_rtk^{rtk}_{10\,Hz} + Doppler\_corr + COG\_corr + Cal\_corr. \tag{1A15}$$

The Doppler correction had to be recomputed since it was not coded properly in the product and the values of the COG_corr and the Cal_corr are respectively equal to $\times\times$ and

××. These values are issued from the analysis of the internal parameters of the Jason-1 ground processing.

Back now to Equations (1A11) and (1A12). Beside the change of definition of the $alt\_trk_{10\,Hz}$ as explained in the previous paragraph, the parameter $\Delta alt_{10\,Hz}$ has also a different definition from the one in the GDR product. In this version of the CMA, it is defined as the difference between the 20 Hz ranges corrected with the USO correction, the Center of Gravity (COG) correction, and the Calibration correction, and the 1 Hz range corrected for all instrumental corrections. Thus, Equation (1A12a) becomes:

$$alt_{10\,Hz} = alt_{1\mathrm{Hz}} + \Delta alt_{10\,Hz} + Doppler\_corr + LookUp\_corr. \tag{1A16a}$$

The *Syst_bias* parameter has not been included in this equation, as it is equal to 0. Given the definition of the parameter $alt\_trk_{10\,Hz}$, Equation (1A12b) becomes:

$$epoch\_rtk_{10\,Hz} = alt_{10\,Hz} - alt\_trk_{10\,Hz} - Sum\_instr\_corr + USO\_corr. \tag{1A16b}$$

These two equations can then be used in conjunction with Equation (1A11).

Equations for Cycle 19 (CMA Version 5.4_06 Up to Version 6.0 Excluded)

The only difference between this version and the previous one is the $\Delta alt_{10\,Hz}$ definition. It is defined as the difference between the 20 Hz ranges corrected with the USO correction, the Center of Gravity (COG) correction, and the Calibration correction, and the 1 Hz range corrected for the same effects. Thus, in the equations of the above paragraph, only Equation (1A16a) has to be changed to Equation (1A12a). All other equations are valid as they are.

Appendix II

Poseidon-1 SSB and Normalization Correction

As reported by AVISO (1996), a normalization process has been performed to get homogeneity between TOPEX and Poseidon-1 user products. It led to separate the −3.7% SWH Poseidon-1 SSB in a −2 to −2.5% SWH BM4 SSB similar to TOPEX plus a −1.7% SWH additional normalization correction incorporated in the sum of the instrumental corrections.

The normalization correction is given by:

$$Norm\_Corr = SWH^{*}(-0.017 + 0.00144^{*}U - 0.000052^{*}U^{2} - 0.00082^{*}SWH), \tag{2A1}$$

where U is the wind speed expressed in m/s. This formula has been applied on the Poseidon-1 data since cycle 138, resulting in a total SSB for Poseidon-1 expressed by the following equation:

$$SSB\_POS1 = SWH^{*}(-0.0373 - 0.00225^{*}U + 0.000097^{*}U^{2} + 0.00183^{*}SWH). \tag{2A2}$$

Appendix III

About Relative SSH Biases

Let's recall that the Jason-1/Poseidon-1 relative retracked SSH bias has been estimated as −9.8 cm, whereas the Jason-1/TOPEX figure is about −11 cm.

What is known from retracking is that: (a) Poseidon-1 waveforms are centered at −34 cm from reference gate, (b) TOPEX waveforms are centered at +1 cm from reference gate, and (c) Jason-1 waveforms are centered at −36 cm from reference gate. Relative tracker SSH biases are thus +2 cm for Poseidon-1 with respect to Jason-1 and +37 cm for TOPEX with respect to Jason-1.

From Figure 17, it appears that the Poseidon-1/Jason-1 tracker SSH difference is of the order of −6 cm while the TOPEX to Jason-1 difference is of the order of 27 cm. These figures are fully consistent with what is known from the tracker algorithms. However, from these figures it is not possible to explain the origin of the relative SSH biases between altimeters at this point of the study.